VOLUME 122 NUMBER 4 DECEMBER 1984

ENCE
ARY

Archives Italiennes de Biologie

A Journal of Neuroscience

U.I.C.
APR 23 1985
LIBRARY

Sci

EDITORIAL BOARD

O. Pompeiano (*Pisa*) CHIEF EDITOR
P. Brodal (*Oslo*)
M. Cuénod (*Zurich*)
E. V. Evarts (*Bethesda*)
J. A. Hobson (*Boston*)
Y. Laporte (*Paris*)
R. Levi Montalcini (*Roma*)
G. Moruzzi (*Pisa*)
E. Mugnaini (*Storrs*)
G. F. Poggio (*Baltimore*)
M. Steriade (*Quebec*)
C. Terzuolo (*Milano*)
N. Tsukahara (*Osaka*)
W. D. Willis (*Galveston*)

ARCHIVES ITALIENNES DE BIOLOGIE

A JOURNAL OF NEUROSCIENCE,
PUBLISHED BY THE UNIVERSITY OF PISA,
WITH THE SUPPORT OF THE CONSIGLIO NAZIONALE DELLE RICERCHE

The *Archives Italiennes de Biologie* publishes original contributions in the fields of Neuroscience, which can include neurophysiology, experimental neuroanatomy and electron microscopy, neurobiology, neurochemistry and behavioral analysis.
Following the tradition of the Archives the contributions can be written in either English or French, according to the choise of the Author. Papers from any country will be considered for publication.

TYPES OF PAPERS

1. **Full-length papers,** reporting results of original research.
2. **Short communications,** reporting on research in progress.
3. **Review articles,** discussing current developments of interest to neuroscientists.
4. **Book reviews,** discussing publications of general interest to neuroscientists.

The *Archives Italiennes de Biologie* is published in quarterly issues by the University of Pisa, Lungarno A. Pacinotti 43, 56100 Pisa, Italy.
The subscription price of Volume 122 (1984) is U.S. $ 40.00 or Lire 60.000 including postages.
Orders which must be accompanied by payment should be sent to: The Administration, Archives Italiennes de Biologie, University of Pisa, Lungarno A. Pacinotti 43, 56100 Pisa, Italy. Claims for missing issues can only be considered if made immediately after receipt of the subsequent issue. Back volumes are also available.

Archives Italiennes de Biologie, *122*: 269-280, 1984.

THE DISTRIBUTION OF SUBSTANCE P IN THE HABENULO-INTERPEDUNCULAR SYSTEM OF THE FROG SHOWN BY AN IMMUNOHISTOCHEMICAL METHOD

M. KEMALI AND V. GUGLIELMOTTI

Istituto di Cibernetica, CNR, Via Toiano 6, 80072 Arco Felice (Naples), Italy

INTRODUCTION

The habenulo-interpeduncular (HAB-ITP) circuit is a unique constellation of structures in the vertebrate central nervous system. Its uniqueness lies in the fact that two paired nuclei, the habenulae (HAB) – located on the right and left side of the epithalamus – converge their fibers, which are gathered together in the two Meinert's fasciculi retroflexes (FR), to a midline single structure, the interpenducular nucleus (ITP) – located in the tegmentum mesencephali. They traverse this nuclei more than once, from one edge to the other, making that zig-zag wiring pattern, well known from the illustrations of Cajal (4), before terminating. The whole HAB-ITP circuit constitutes the inner ring – the phylogenetically oldest portion – of the limbic system.

Few changes have occurred in the HAB-ITP system during the phylogenetic history of the vertebrate brain and this system in its essence is considered one of the most conservative structures from cyclostomes to man (9).

The modifications which occurred during the evolution of the central nervous system are mainly in the epithalamic region. They concern the pineal complex with which the HAB establish connections modifiable during phylogenesis. These modifications are considered by early anatomists (12, 14, 16), and by more recent anatomists using tracing techniques such as horseradish peroxidase (HRP) (7, 21) to be the probable source of the morphologic asymmetry of the habenular nuclei in lower vertebrates.

Here we only take into consideration the HAB-ITP system of the frog and disregard the extracranial (frontal organ) and the intracranial (epiphysis) portions of the pineal complex. The HAB of the frog are subdivided into dorsal and ventral nuclei which correspond to be medial and lateral HAB respectively of mammals (2). In addition, the dorsal HAB of the frog are strikingly asymmetric, the left being more lobated than the right (19).

The projections of the HAB-ITP system have been studied by means of HRP (21, 23) and cobalt tracing techniques (24) and these studies have underlined the differential connections established by the various parts of the system. However, using HRP, the two FR have been found to be of the same size (22). In the present paper we have tried to correlate the well established asymmetry of the frog HAB with the immunolocalization of substance P (SP).

There is experimental evidence that SP participates in neuronal communication either as a conventional neurotransmitter or as a modulator (27). The components of the HAB-ITP system have neurons and fibers positive to SP in all the species studied (5, 10, 26, 31) raising the possibility of a nociceptive function of this circuit.

In the frog such information is scarse. Inagaki *et al.* (13), in an immunofluorescence study on the overall distribution of SP in the frog *Rana catesbiana* report SP positive fibers in the ITP but do not mention the other components of the complex, while perikarya showing SP-like immunoreactivity were reported in the HAB and ITP of the newt (31).

In the present paper we demonstrate, by means of the peroxidase-antiperoxidase (PAP) method that SP is distributed widely in the HAB-ITP system of the frog and that this distribution is asymmetric[1].

MATERIAL AND METHODS

The immunoperoxidase PAP technique (30) was applied to 12 adult frogs of the species *Rana esculenta* of both sexes. Two of the frogs were treated with colchicine (Carlo Erba) (10 mg/100 gm body weight dissolved in 0.9% NaCl) by intraperitoneal injection 48 hours prior to the immunohistochemical procedure.

The twelve frogs were anaesthetized with tricaine methanesulphonate (MS 222. Sandoz) 1: 3.000 and perfused transcardially with 20 ml of 4% formaldehyde in 0.1M phosphate buffer at pH 7.4, at 4° C. The HAB and the ITP (sometimes a single piece containing both structures) were rapidly removed, postfixed for 3 hours at 4° C in the same fixative used for the perfusion and stored for 2 days in 20% sucrose in 0.1M phosphate buffer.

Complete serial transverse and horizontal sections of the HAB and ITP were cut 12 μm thick in a cryostat (Reichert-Jung Mod. 2700). Three groups of 4 sections each were mounted on slides pretreated with chrome alum gelatin. The slides were rinsed at room temperature for 30 min in phosphate buffered saline [PBS] and for further 5 min in PBS/T (PBS plus 0.3% Triton X 100), the latter buffer being used for diluting all the incubation sera. All the rinsing steps were carried out keeping the slides on a slow horizontal agitator. The incubations were carried out in a humid atmosphere at room temperature except for the primary antiserum (SP) which was incubated for 90 min at 37° C.

The slides were first incubated for 10 min with normal swine serum diluted 1: 5, then with SP antiserum (Minnesota Nuclear Corp., Stillwater, Minnesota, USA), diluted 1: 300 and 1: 400, following which they were each given three 5 min rinses with PBS/T and then incubated for 30 min with swine anti-rabbit immunoglobulin diluted 1: 30. After having been rinsed three times for 5 min each in PBS/T, the sections were incubated for 30 min with PAP complex (HRP/rabbit anti-HRP) diluted 1: 30, then rinsed once for 5 min with PBS, twice for 5 min each with 0.05M Tris buffer containing 0.9% NaCl, pH 7.6, prior to the last step, carried out in the dark room, which was the incubation for 15-20 min in 0.067% 3, 3′-diaminobenzidine 4HCl-$2H_2O$ in 0.05M Tris HCl buffer pH 7.6 containing 0.003% H_2O_2. The slides were then dehydrated in graded alcohols, cleared in xylene and mounted in Permount for light microscope examination.

---

[1] Presented in part at the 7th European Neuroscience Meeting, Hamburg, Germany, Sept. 1983.

Specificity of the immunoreaction was established by showing absence of diaminobenzidine staining in sections processed in parallel but incubated with primary antiserum preabsorbed, 24 hours before the while histological procedure with SP (100 μg/ml), or by deleting the incubation with the primary antiserum.

The topography of the SP immunoreaction positive cell bodies was compared with a Nissl-stained standard series of the frog's Rana esculenta brain.

RESULTS

The results of our study are illustrate in Fig. 1-4 which are sections from frogs not treated with colchicine. In fact the colchicine-treated frogs did not add any further information to our study.

The cytoarchitecture of the HAB is illustrated in Fig. 1 *a*, which shows a frontal section of the frog brain stained according to the Nissl method. The boundary between the dorsal and ventral HAB is indicated in the figure by the arrows. The different cytoarchitectonic distribution of the cells of the dorsal and ventral HAB are apparent. In the dorsal HAB a few rows of cells encircle, like a ring, the neuropil while cells sparsely distributed characterize the ventral HAB. In addition, the dorsal HAB is asymmetric, only the left one being subdivided into two subnuclei (a medial and a lateral) as shown in Fig. 1 *a*.

After the immunohistochemistry procedure (Fig. 1 *b*), the cells of the dorsal HAB show SP-like immunoreactivity which can be seen as a funnel confined to the pole of the cell from which the processes directed to the neuropil arise. This peculiar pattern is probably due to the fact that the cells of the dorsal HAB as seen in the electron microscope (20), have a very large nucleus and various cytoplasmic organelles confined to the cellular pole facing the neuropil.

As illustrated in Fig. 1 *b*, the SP-like immunoreactivity is distributed asymmetrically in the HAB of the two sides of the brain. In fact the dorsal right HAB and the lateral subnucleus of the dorsal left HAB show their cells positive to the SP-like immunoreactivity, while the medial subnucleus of the left dorsal HAB does not give such an immunohistochemical response. It must be pointed out, however, that a small portion of the right dorsal HAB facing the third ventricle, also lacks SP immunoreactivity.

The medial subnucleus of the left dorsal HAB has a few fibers with SP-like immunoreactivity in its neuropil (Fig. 2 *a*), while the ventral HAB in both sides show numerous SP-like immunoreactive terminals (Fig.s 2 *b*).

The asymmetric distribution of SP-like immunoreactivity is visible also in the fibers of the FR, the main pathway connecting the HAB to the ITP. In this case the FR of the left side (Fig. 2 *c*) shows less SP immunoreactive fibers than the FR of the right side (Fig. 2 *d*).

The other nucleus of the HAB-ITP system, the ITP, shows fibers, terminals and a few parikarya with SP-like immunoreactivity. There is no asymmetry in the distribution of SP immunoreactive fibers within the ITP. This is apparent from Fig.

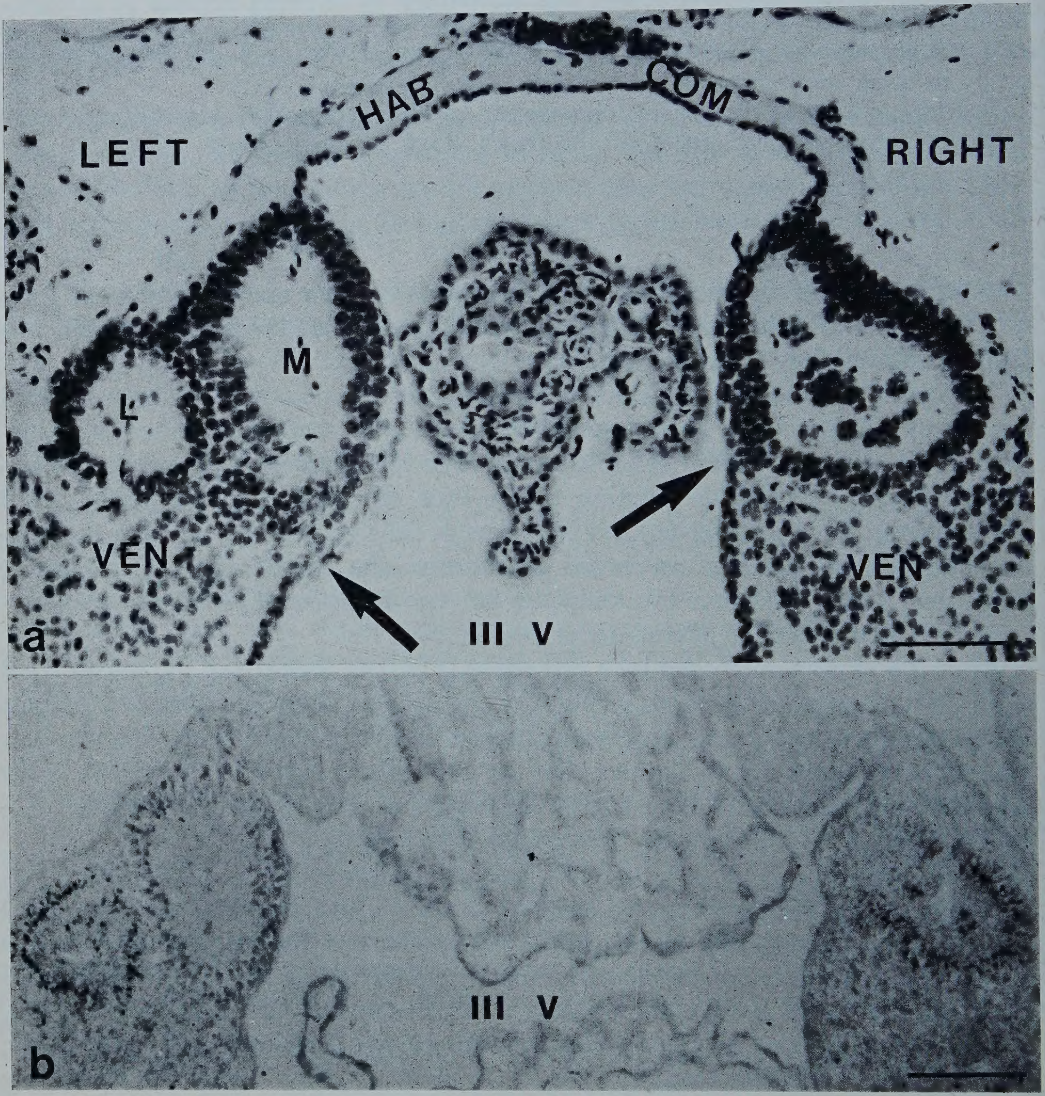

Fig. 1. – *Transverse sections of the epithalamus of the frog at the level of the HAB.*

a: Nissl stained section. The arrows indicate the boundary between dorsal and ventral HAB (VEN). Note the asymmetry of the dorsal HAB, the left one being formed by two subnuclei, a medial, close to the ventricle, and a lateral. HAB COM = habenular commissure; lateral (L) and medial (M) subnucleus of the left dorsal HAB.

b: SP-like immunoreactivity in the right dorsal HAB and in the lateral subnucleus of the left dorsal HAB. Note that the portion of the right dorsal HAB facing the third ventricel, shows no SP immunoreactivity.

III V = third ventrice. Calibration bar = 100 μm.

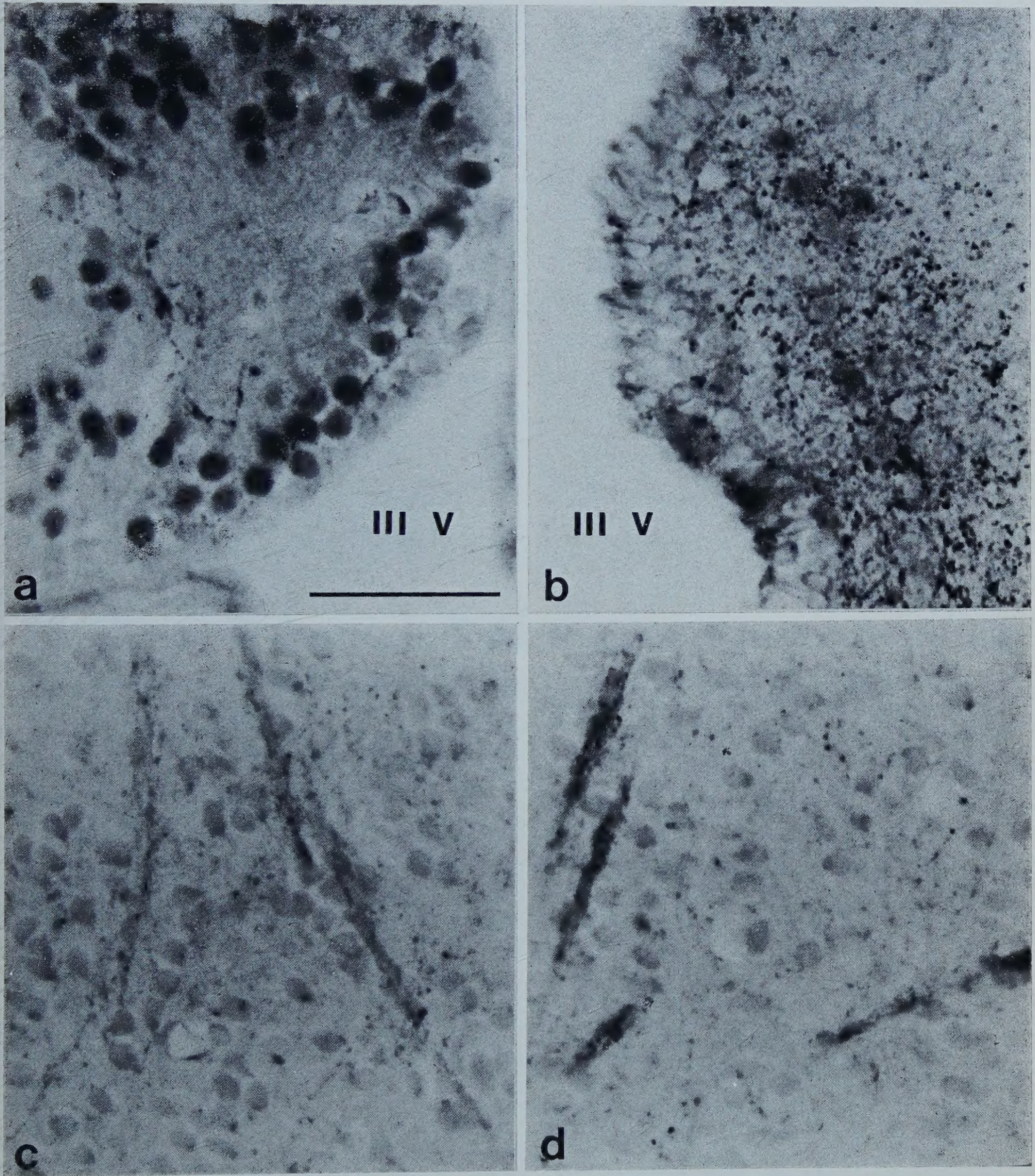

Fig. 2. – *SP-like immunoreactive fibers and terminals in the HAB and FR.*

a: SP-like immunoreactive fibers in the medial subnucleus of the left dorsal HAB.
b: SP-immunoreactive terminals in the ventral HAB.
c and *d*: SP-like immunoreactive fibers in the left and right FR respectively.
III V = third ventricle. Calibration bar = 50 μm.

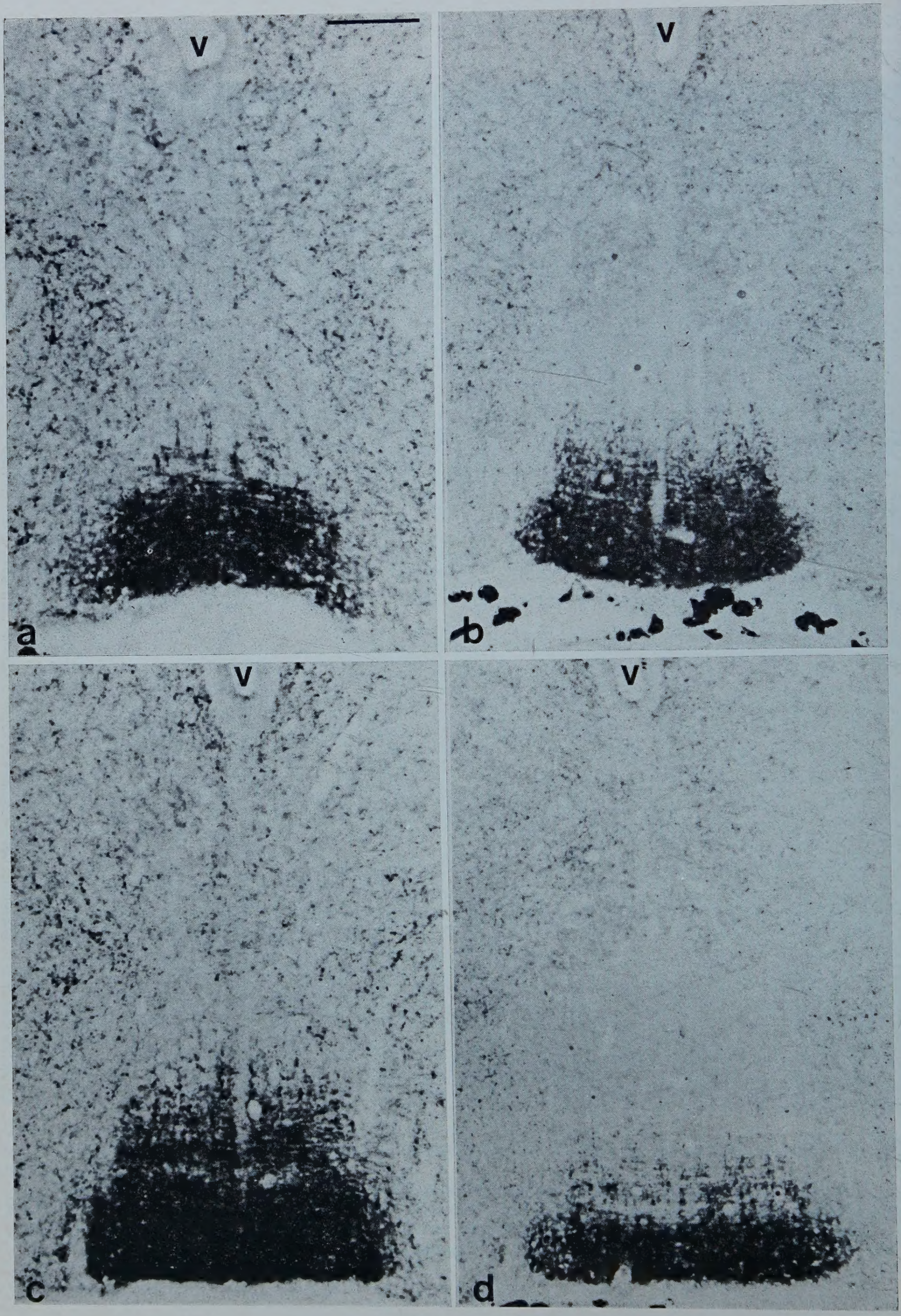

Fig. 3.

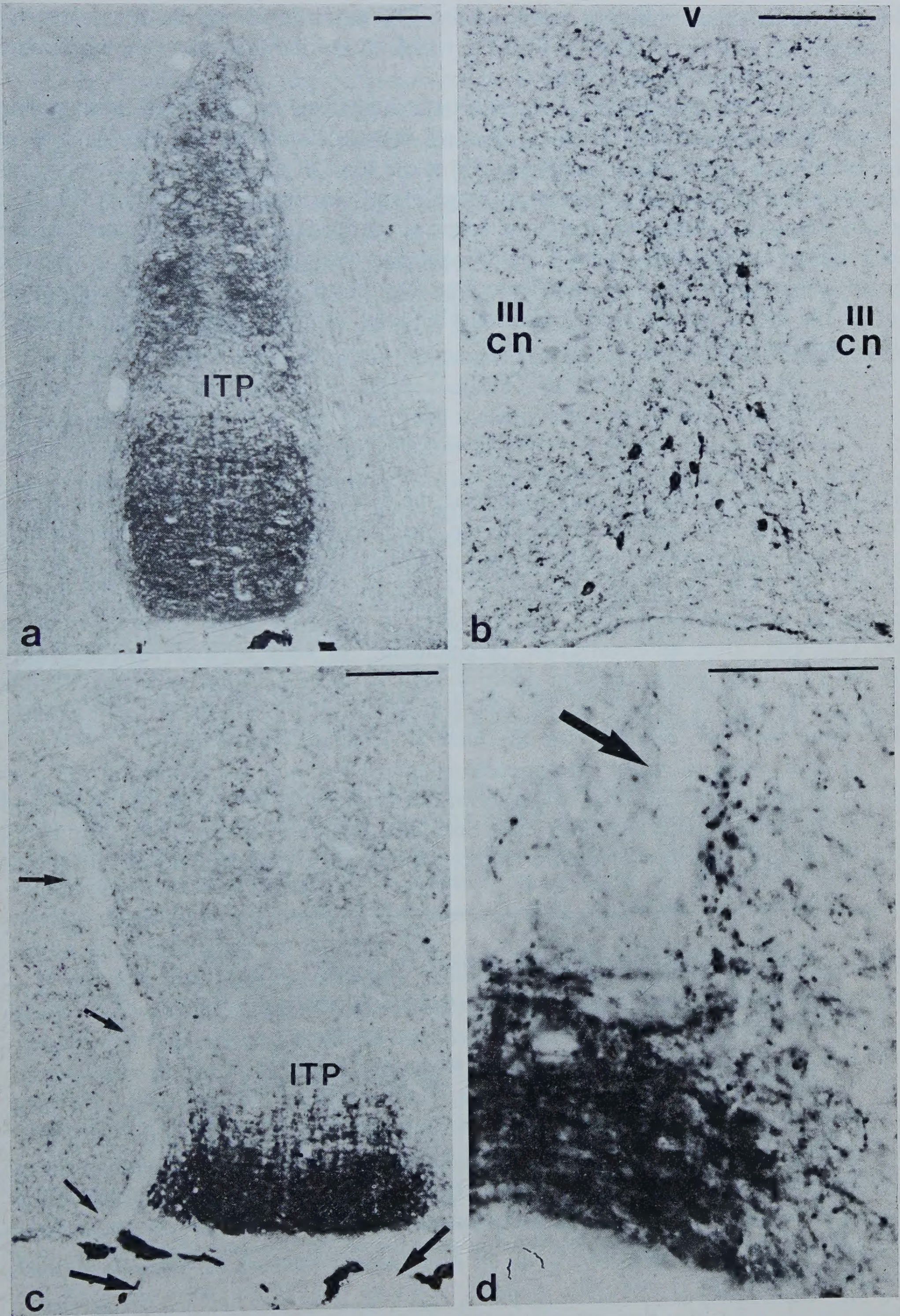

Fig. 4.

3 (*a-d*) which shows different levels of the ITP cut transversely in the rostro (*a*) to caudal (*d*) direction and from Fig. 4 *a*, which shows the ITP cut in the horizontal plane.

In addition, we were able to demonstrate a nucleus of scattered cells with strong SP-like immunoreactivity which is located rostro-dorsally to the ITP shown in Fig. 4 *b* which represents a transverse cut at the level of the third cranial nerve nuclei. The ITP of the frog is crossed by large blood vessels (small arrows in Fig. 4 *c*) which run on the right and left lateral edges of the nucleus and which communicate with the two huge blood vessels on the subpial ventral surface of the brain, the latter being shown cut transversely in Fig. 4 *c* (large arrows). At higher magnification the blood vessels which cross the ITP show numerous SP-like immunoreactive terminals (Fig. 4 *d*).

DISCUSSION

The results of our study demonstrate that the HAB-ITP system of the frog has a rather extensive distribution of SP immunoreactive elements which is in accordance with the immunohistochemical findings reported on the same system of mammals (5, 10, 26). They are in accordance with the results of Inagaki *et al.* (13) who, by means of immunofluorescence demonstrated in the frog *Rana catesbiana* SP in the ITP and, after administration of colchicine, in cells located rostro-dorsally to the ITP. Our results show in addition that in the frog *Rana esculenta* SP-like immunoreactivity is present, in various degrees, in all the HAB-ITP components. The same has been reported for the newt a urodele amphibian (31).

The cells which show the immunohistochemical reaction are located in the dorsal HAB and in the ITP area, while terminals are located in the ventral HAB and in the ITP where numerous fibers have been demonstrated as also in the FR. From this we deduce that, with reference to this peptidergic system, the dorsal HAB and

---

Fig. 3. – *SP-like immunoreactive fibers and terminals in the ITP.*

Transverse sections of the ITP cut in a rostro-caudal (a-d) direction.
Calibration bar = 100 μm.

Fig. 4. – *SP-like immunoreactive fibers, terminals and cells in the ITP.*

a: Horizontal section of the ITP showing heavy SP-like immunoreactive fibers. Calibration bar = = 100 μm.

b: Transverse section of the ventral tegmentum showing a nucleus of SP-like immunoreactive cells located rostrodorsally to the ITP. The cut was at the level of the nucleus of the 3rd cranial nerve (III cn). V = cerebral aqueduct. Calibration bar = 100 μm.

c: Transverse section of the mesencephalic tegmentum at the level of the ITP which shows SP-like immunoreactivity. The small arrows indicate a blood vessel cut longitudinally while the large arrows indicate, on the subpial ventral surface of the brain, two large blood vessels cut transversely. Calibration bar = 100 μm.

d: High magnification of a portion of the ITP showing a blood vessel (arrow) with SP-like immunoreactive terminals on its surface. Calibration bar = 5 μm.

some elements of the ITP area are efferent structures while the ventral HAB and the remainder ITP are afferent structures.

The application of tracing techniques to the HAB-ITP system of the frog demonstrated that HRP injected into the dorsal HAB revealed, beyond various efferences, a projection to the ITP (23) while the same injection of HRP into the ITP demonstrated labeled cells in the dorsal HAB (21). Injection of cobalt in the FR at the level of the thalamus demonstrated labeled cells in the dorsal HAB as well as in the ventral HAB (24). This implies that the FR, along its pathway, collects fibers from and projects fibers to several structures. Since no SP-like immunoreactive cells were found in the ventral HAB, it seems that the portion of the FR which originates in the ventral HAB does not contain SP.

In addition, HRP applied to the rat lateral HAB (equivalent to the frog ventral HAB) labeled some cells in a midline nucleus located in the ventro-tegmental area closely related to the FR and ITP. This nucleus was named the interfascicular nucleus (28) and biochemical studies demonstrated that it gives a contribution to a mesohabenular dopamine projection (29). Also the application of fluorescent retrograde tracers demonstrated in the rat a projection to the lateral HAB from a portion of cells located in the ventral tegmental area (1).

We cannot exclude that the SP-like immunoreactive cells demonstrated in our study, which are located rostro-dorsally to the ITP, project to the ventral HAB, where numerous SP-like immunoreactive terminals are present. Furthermore, the possibility that these same cells might represent a portion of the ventral tegmental area, which is a rather complex area containing groups of neurons with dopamine (6) and with peptides such as cholecystokinine (11) and enkephalin (15) remains to be elucidated.

Beyond the demonstrations of the portion of the HAB-ITP system which is peptidergic, our study is also in favour of an asymmetric distribution of SP-like immunoreactivity in the frog HAB-ITP system. In fact the dorsal HAB show SP-like immunoreactive cells, although of low intensity in the right and in the lateral portion of the left dorsal HAB, while the number of SP-like immunoreactive fibers is greater in the right than in the left FR.

If we take into consideration the total cell population of the frog right dorsal HAB which is 8,500 and of the lateral subnucleus of the dorsal left HAB which is 4,470 (3) then we can correlate the larger right FR to the larger cell population of the right dorsal HAB, even if a small portion of its cells, those facing the third ventricle, have no SP immunoreactivity.

The immunohistochemical asymmetry is not apparent in the ITP which shows a strong SP-like immunoreactivity distributed equally throughout its length. This is understandable when one considers the peculiar zig-zag wiring of the fibers which traverse the ITP from one edge to the other through the midline more than once before terminating. Although in the ITP of the rat a left-right pairing of the crest synapses has been interpreted as convergence of afferents arising in the right and left HAB (25), the peculiar wiring pattern of the fibers in the frog ITP may hide or counterbalance the asymmetry in SP-like immunoreactive fibers originating in the HAB and distributing to the ITP through the FR.

An histochemical asymmetry has been reported in the HAB of a lizard (8) where SP-like immunoreactive processes occurred in the left medial HAB and not in the right HAB. Besides the frog, we described a morphological asymmetry occurring also in the HAB of a lizard (18). So it seems that the morphological and the histochemical asymmetries are concomitant features in the HAB of low vertebrates.

In conclusion, the frog might share with mammals the same HAB-ITP SP-like immunoreactive pattern with the exception of the asymmetry. The latter feature parallels, from the histochemical point of view in a general way the morphological asymmetry of the HAB which has not yet been clarified functionally.

Beyond the asymmetric distribution of SP-like immunoreactivity in the HAB-ITP system of the frog other aspects remain to be explained, as for instance the meaning of SP-like immunoreactive terminals on the blood vessels which traverse the ITP. This is a structure which according to electron microscopic findings was postulated to have a neurosecretory function (17).

SUMMARY

The distribution of substance P(SP)-like immunoreactivity was studied in the habenulo-interpeduncular (HAB-ITP) complex of the frog *Rana esculenta* by means of the immunohistochemical peroxidase-antiperoxidase (PAP) method. The HAB of the frog were subdivided into dorsal and ventral nuclei, corresponding to the medial and lateral HAB of mammals respectively. In addition, the dorsal HAB of the frog were morphologically asymmetric, since only the left has a lateral and a medial subnucleus.

SP-like immunoreactive cells were found in the right dorsal HAB, in the lateral subnucleus of the left dorsal HAB and in a nucleus of scattered cells located rostrodorsally to the ITP. However, the medial subnucleus of the left dorsal HAB and a portion of the right dorsal HAB facing the 3rd ventricle, did not show SP immunoreactivity. Immunoreactive fibers were found in the medial subnucleus of the left dorsal HAB, in the two fasciculi retroflexes and in the ITP. Moreover, immunoreactive terminals were observed in the ventral HAB of both sides, in the ITP and on the blood vessels which cross the ITP.

It is assumed that a portion of the fibers connecting the various structures of the HAB-ITP complex belongs to the SP peptidergic system as suggested for mammals. However, in contrast to the mammals, the results on the frog are in favour of an histochemical asymmetry of the SP-like immunoreactivity, since a different distribution of this peptide was found between the right and left side of the brain. Such histochemical asymmetry was less pronounced than the morphological asymmetry and its functional meaning is unknown.

Acknowledgements. — The authors are very grateful to Dr. H. P. Lorez, Hoffman-La Roche, Basel, for his valuable suggestions which have permitted the realization of this paper.

REFERENCES

1. Albanese, A. and Minciacchi, D. Organization of the ascending projections from the ventral tegmental area: a multiple fluorescent retrograde tracer study in the rat. *J. comp. Neurol.*, **216**: 406-420, 1983.
2. Beccari, N. *Neurologia Comparata*, Firenze, Sansoni, 772 pp., 1943.
3. Braitenberg, V. and Kemali, M. Exceptions to bilateral symmetry in the epithalamus of lower vertebrates. *J. comp. Neurol.*, **138**: 137-146, 1970.
4. Cajal Ramon y S., *Histologie du Systéme Nerveux de l'Homme et des Vertébrés.* Vol. 2, Paris, Maloine, 1911.
5. Cuello, A. C., Emson, P. C., Paxinos, G. and Jessell, T. Substance P containing and cholinergic projections from the habenula. *Brain Res.*, **149**: 413-429, 1978.
6. Dahlstrom, A. and Fuxe, K. Evidence for the existence of monoamine-containing neurons in the central nervous system. I. Demonstration of monoamines in the cell bodies of brain stem neurons. *Acta physiol. scand.*, Suppl. **232**: 1-55, 1964.
7. Eldred, W. D., Finger, T. E. and Nolte, J. Central projections of the frontal organ of Rana pipiens as demonstrated by the anterograde transport of horseradish peroxidase. *Cell Tissue Res.*, **211**: 215-222, 1980.
8. Engbretson, G. A., Brecha, N. and Reiner, A. Substance P-like immunoreactivity in the parietal eye visual system of the lizard Uta stansburiana. *Cell Tissue Res.*, **227**: 543-554, 407 pp., 1982.
9. Herrick, C. J. *The Brain of the Tiger Salamander.* Chicago, University of Chicago Press, 407 pp., 1984.
10. Hökfelt, T., Elde, R. P., Johansson O., Ljungdahl, A., Schultzberg, M., Fuxe, K., Goldstein, M., Nilsson, G., Pernow, B., Terenius, L., Gauten, D., Jeffcoate, S. L., Rehfeld, J. and Said, S. Distribution of peptide containing neurons. Pp. 39-66. In Lipton, M. A., Di Mascio, A. and Killam, K. F. (Eds.) *Psychopharmacology: A Generation of Progress.* New York, Raven Press, 1978.
11. Hökfelt, T., Rehfeld, J. D., Skirboll, B., Ivemark, B., Goldstein, M. and Markey, K. Evidence for coexistence of dopamine and CCK in mesolimbic neurones. *Nature*, **285**: 476-478, 1980.
12. Holmgren, N. and Van der Horst, C. J. Contribution to the morphology of the brain of Ceratodus. *Acta Zool.*, **6**: 59-165, 1925.
13. Inagaki, S., Senba, E., Shiosaka, S., Takagi, H., Kawai, Y., Takatsuki, K. Sakanaka, M., Matsuzaki, T. and Toyama, M. Regional distribution of substance P-like immunoreactivity in the frog brain and spinal cord: immunohistochemical analysis. *J. comp. Neurol.*, **201**: 243-254, 1981.
14. Jansen, J. The brain of Myxine glutinosa. *J. comp. Neurol.*, **49**: 359-507, 1930.
15. Johnson, R. P., Sar, M. and Stumpf, W. E. A topographic localization of enkephalin on the dopamine neurons of the rat substantia nigra and ventral tegmental area demonstrated by combined histo-fluorescence-immunohistochemistry. *Brain Res.*, **194**: 566-571, 1980.
16. Johnston, J. B. The brain of Petromyzon, *J. comp. Neurol.*, **12**: 1-86, 1902.
17. Kemali, M. The interpeduncular nucleus (ITP): ultrastructure data in favour of a possible neurosecretory activity. *Cell Tissue Res.*, **178**: 83-96, 1977.
18. Kemali, M. and Agrelli, I. The habenulo-interpeduncular nuclear system of a reptilian representative Lacerta sicula. *Z. mikr.-anat. Forsch.*, **85**: 325-333, 1972.
19. Kemali, M. and Braitenberg, V. *Atlas of the Frog's Brain.* Heidelberg, Springer Verlag, 74 pp., 1969.
20. Kemali, M. and Guglielmotti, V. An electron microscope observation of the right

and the two left portions of the habenular nuclei of the frog. *J. comp. Neurol.*, **176**: 133-148, 1977.

21. KEMALI, M. and GUGLIELMOTTI, V. The connections of the frog interpeduncular nucleus (ITP) demonstrated by horseradish peroxidase (HRP). *Exp. Brain Res.* **45**: 349-356, 1982.
22. KEMALI, M. and GUGLIELMOTTI, V. Quantitative evaluation of the number of fibers in the right and left fasciculus retroflexus using horseradish peroxidase. *Z. mikr.-anat. Forsch.*, **96**: 750-754, 1982.
23. KEMALI, M., GUGLIELMOTTI, V. and GIOFFRÈ, D. Neuroanatomical identification of the frog habenular connections using Peroxidase (HRP). *Exp. Brain Res.*, **38**: 341-347, 1980.
24. KEMALI, M. and LAZAR, G., Cobalt injected into the right and left fasciculi retroflexes clarifies the organization of this pathway. *J. comp. Neurol.,* 1984, in press.
25. LENN, N. J., WONG, V., and HANNIL, G. S. Left-right pairing at the crest synapses of rat interpeduncular nucleus. *Neuroscience*, **9**: 383-389, 1983.
26. MROZ, E. A., BROWNSTEIN, M. J., and LEEMAN, S. E. Evidence for substance P in the habenulo-interpeduncular tract. *Brain Res.*, **113**: 597-599, 1976.
27. PERNOW, B. Substance P. *Pharmacol. Rev.*, **35**: 85-141, 1983.
28. PHILLIPSON, O. T. and GRIFFITH, A. C. The neurones of origin for the mesohabenular dopamine pathway. *Brain Res.*, **197**: 213-218, 1980.
29. PHILLIPSON, O. T. and PYCOCK, C. J. Dopamine neurones of the ventral tegmentum project to both medial and lateral habenula. *Exp. Brain Res.*, **45**: 89-94, 1982.
30. STERNBERGER, L. A. *Immunocytochemistry.* Inglewood Cliffs, N. J., Prentice Hall, 246 pp., 1974.
31. TABAN, C. H. and CATHIENI, M. Distribution of substance P-like immunoreactivity in the brain of the newt (Triturus cristatus). *J. comp. Neurol.*, **216**: 453-470, 1983.

Archives Italiennes de Biologie, 122: 281-300, 1984.

EXPERIMENTAL STUDIES ON DIFFERENT THRESHOLDS FOR EPILEPTIFORM ACTIVITY

T. YAMAUCHI[1], S. E. NEWMAN[2] AND C. AJMONE-MARSAN[3]

Clinical Neurosciences Branch, National Institute of Neurological
and Communicative Disorders and Stroke,
National Institutes of Health, Bethesda, MD 20205, U.S.A.

INTRODUCTION

It is well known that there are low and high seizure threshold regions in the brain. However, the mechanisms underlying these differences in threshold are still unclear. One question is whether different seizure thresholds result from individual cell phenomena or from cell populations (synaptic connection) in different neuronal structures. To clarify this problem, effects of penicillin on single cell or cell population were examined in both hippocampus (low seizure threshold) and olfactory bulb (high seizure threshold).

METHODS

Adult cats (2.0-3.5 kg) were anesthetized with ketamine (10-20 mg/kg) and/or ether for sugery. A small amount of sodium thiopental was administered and long-acting procaine was repeatedly infiltrated into the wound margins and pressure points during experiment. Routine tracheotomy and cannulation were performed. Cats were paralyzed with gallamine triethiodide and artificially ventilated with humidified 0_2 by Harvard respirator.

Arterial blood pressure, electrocardiogram, and body temperature were monitored continuously. Bilateral pneumothorax and axial suspension were performed to prevent respiratory and pulsatile movements.

The olfactory bulbs and frontal cortex were cautiously exposed, and the hippocampus was exposed by suction decortication of one cerebral hemisphere. Surface potentials were recorded by silver ball tipped electrodes, and extracellular potentials were recorded by using 5-barrel microelectrodes whose tip size was 6-9 μ in diameter. Hippocampal pyramidal cells were identified by electrical stimulation (11, 22). Silver tipped stimulation electrodes were placed under direct vision on the fimbria or the alveus. Stimulation parameters were 0.05-0.10 msec square-wave pulses of 0.2-0.3 Hz. Hippocampal surface activity was recorded from bipolar silver electrodes attached to a pressor foot which reduced pulsation artifact. The olfactory bulb mitral cells were identified by the antidromic spike discharge occurring within 2 msec after electrical stimulation of their centripetal part in the ipsilateral lateral olfactory tract (7). The lateral olfactory tract was stimulated by co-axial bipolar needle electrode (tip diameter 0.5 mm) with the same stimulation parameters as described at the hippocampal surface stimulation.

---

[1] Present address: Hokkaido University School of Medicine, Dept. of Psychiatry and Neurology, Sapporo, 060, Japan.

[2] Present address: Detroit Institute of Physical Medicine and Rehabilitation. 25811, Mile Road, Southfield, MI. 48034, U.S.A.

[3] Present address: University of Miami, School of Medicine, Dept. of Neurology, EEG Laboratory, Jackson Memorial Hospital, Miami, Fla. 33136, U.S.A.

The central barrel of a microelectrode was filled with 4 *M* NaCl and used for recording (1-3 MΩ). Each of the side barrels was filled with one of the following substances: 1) D-L-homocysteic acid (0.2 *M*, pH-7 adjusted with NaOH, 50-150 MΩ), 2) γ-aminobutyric acid [1 *M*, pH-3 adjusted with HCl, 30-100 MΩ], or 3] benzyl penicillin (0.3 *M*, pH-7 adjusted with either NaOH or citric acid, 20-70 MΩ).

If the spontaneous unit firing rate was less than 10 spikes/sec, it was maintained between 10 and 20 spikes/sec with D-L-homocysteic acid (DLH). After a stable and suitable unit for analysis was recorded, penicillin was applied either iontophoretically passing through one barrel of the multibarrel micro-electrode, or topically.

Current was passed by a multichannel microiontophoretic apparatus (20). A 25 nA holding current for drugs, and a 50 nA holding current for penicillin was used. Since artifacts tended to occur with ejecting currents in excess of 500 nA, currents less than – 100 nA were selected for the penicillin electrode. Also, one of the side barrels of 5-barrel electrode was filled with 3*M* NaCl and functioned as a current summating balance electrode to reduce current related artifacts.

Penicillin was topically applied to the dorsal hippocampus or surface of olfactory bulb adjacent to the microelectrode by placing a 1 mm^3 Gelfoam pledget, or a 1 mm^2 section of filter paper previously soaked in a sodium penicillin G (Sigma) solution of 100,000 IU/ml; or a small amount of penicillin powder was gently placed on the surface using the tip of a polyethylene tube with an internal diameter of 1.15 mm.

Firing rates were calculated from analogue pulses, generated by an amplitude time discriminator system. This permitted preselected spike characteristics to trigger the rate meter. Firing pattern also could be easily calculated by the interval of unit discharge. Results were recorded on a Brush Accuchart ink writer output.

RESULTS

Changes in single cell activity after penicillin application were examined under three main aspects, *i.e.* changes in 1) firing rate, 2) GABA inhibitory effect and 3) post-discharge inhibition.

EFFECTS OF PENICILLIN IONTOPHORESIS ON A SINGLE CELL.

I. *Hippocampus.*

Activity from 96 extracellular hippocampal pyramidal cells was recorded in 56 cats. 58 units were identified as pyramidal cells by electrical stimulation. The range of latencies following electrical stimulation of alveus or the fimbria was 0.2 to 2.0 msec. Most of the pyramidal cells were located 0.3 to 0.6 mm below the surface of the hippocampus. The remaining 38 units did not respond to the electrical stimulation. The following findings refer to the pyramidal cell group, but the electrophysiological results were essentially similar in both the identified pyramidal and the unidentified cells.

1. *Firing rates.* — Penicillin was applied iontophoretically to each cell and the change in the firing rate was examined. Application of – 20 to – 100 nA penicillin resulted in a progressive increase in firing rates of most cells (Fig. 1 *B*). In order to quantitatively evaluate the change of firing rate following – 50 nA penicillin iontophoresis, increment of a total number of unit discharge in 60 sec was counted and compared with control one at each minute and expressed as percent change of firing rate. 49 of 52 cells showed increase in firing rate (Fig. 1 *A*). The remainder demonstrated a fluctuating rate of firing. In only three of the cells either firing rate did not change or it was decreased.

The firing rate increased within 1 minute of the onset of penicillin iontophoresis in 65.3% of the cells: and within 2-6 minutes in the remainder. Within 3 minutes

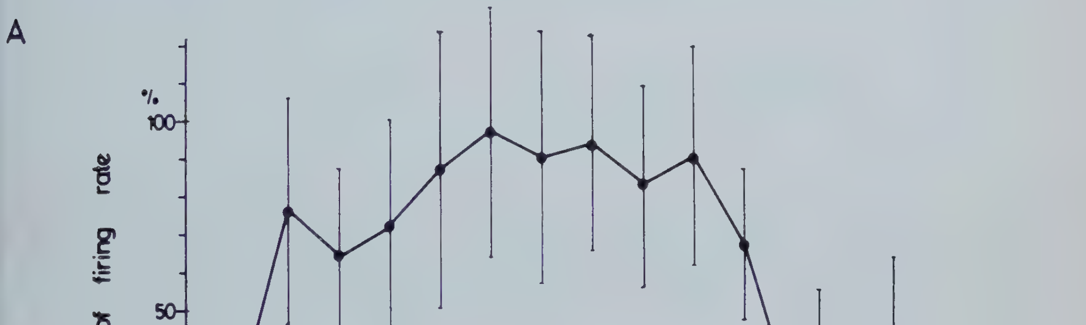

Fig. 1. – *Changes in the firing rate during penicillin iontophoretic application (hippocampus).*

A: The percent change of firing rate is represented by the mean value and standard error of 49 units. Total number of unit discharge was counted for 60 sec. and change of firing rate was expressed as the ratio to control firing rate (before penicillin application). Note increase of firing rate during penicillin (– 50 nA) iontophoresis. *B*: Example of changes in firing rate is presented as a rate meter analysis. Firing rates increase during continuous penicillin iontophoresis (– 50 nA).

after ending penicillin iontophoresis the firing rates returned to the control levels. These results were similar whether in the presence, or absence of DLH.

The firing pattern demonstrated no cluster firing during penicillin iontophoresis even if penicillin was applied continuously for 1 hour or longer (6 cells).

2. *GABA effects.* — *a*) Continuous GABA iontophoresis: GABA was applied continuously for 8-10 min to 5 cells and the effect of penicillin on the inhibitory response to GABA was studied. Continuous iontophoretic GABA application (3-30 nA) produced almost complete suppression of spontaneous or DLH induced firing. However, 1-2 minutes after the onset of penicillin iontophoresis the unit firing reappeared and gradually increased in frequency. Within a few minutes following the cessation of penicillin iontophoresis, GABA inhibitory action returned to the control firing level (Fig. 2 *B*).

b) Intermittent GABA iontophoresis: GABA was applied intermittently to a

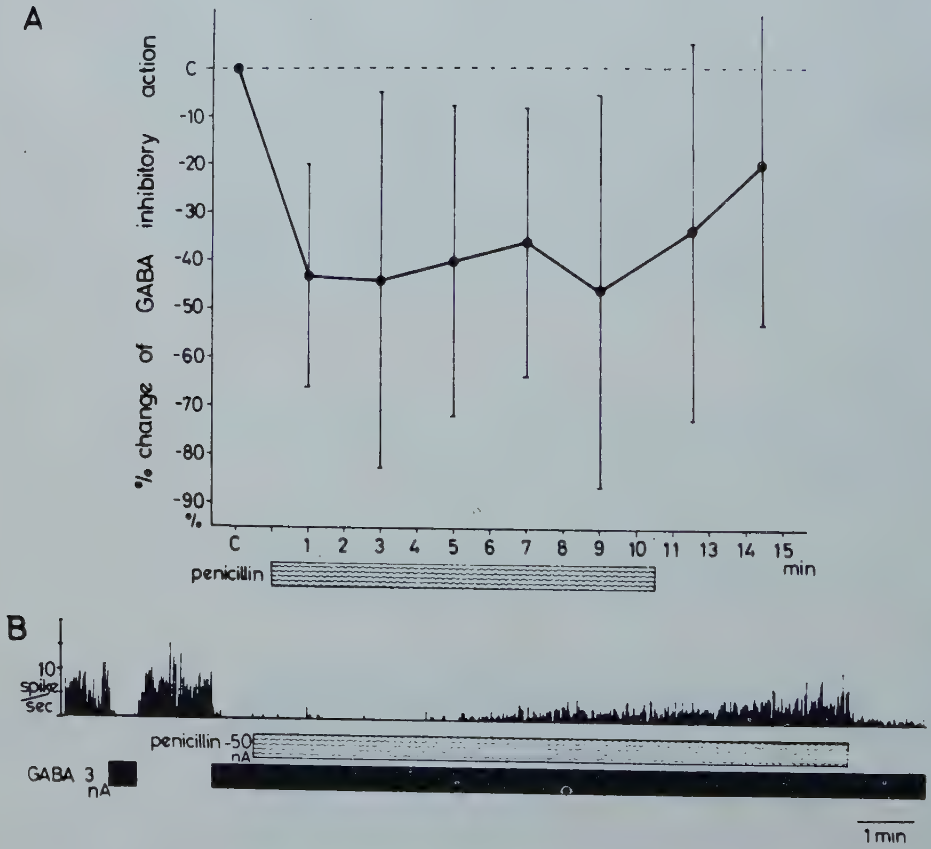

Fig. 2. – *Effects of penicillin on GABA inhibitory action (hippocampus).*

A: The percent change of GABA inhibitory action is illustrated by the mean value and standard error of 21 units. GABA inhibitory action is expressed as suppression of firing rate by GABA application (see text). GABA inhibitory action decreased during penicillin application. *B*: Penicillin and GABA interaction is presented as a rate meter analysis. GABA inhibition is gradually overcome by penicillin.

cell during penicillin iontophoresis. GABA at the control dose of 3-30 nA completely suppressed unit firing in 88.9% of 54 cells which were tested. However, during penicillin iontophoresis these same doses of GABA either required a longer time interval for complete suppression of firing, or failed to completely suppress unit firing during a time interval equal to or less than the control interval in most cells.

In order to quantitatively evaluate the change of GABA inhibitory effects, the following procedure was performed: GABA iontophoresis was adjusted to cause complete inhibition of cell firing within 30 sec. This effective dose of GABA was repeatedly applied to a cell before (control) and at 1, 3, 5, 7 minute of penicillin continuous application (– 50 nA) and also 1 and 3 minute after cessation of penicillin.

From this procedure the total number of unit discharge in 30 sec during GABA application prior to, during, and after penicillin was determined. Changes of GABA inhibitory action was expressed by using following formula:

$$\frac{\begin{array}{c}\text{Firing rate during GABA}\\ \text{before penicillin}\end{array} - \begin{array}{c}\text{Firing rate during GABA}\\ \text{during or after penicillin}\end{array}}{\text{Firing rate during GABA before penicillin}} \times 100$$

The summary of results of the changes in the inhibitory effect of GABA in 21 cells in presented in Fig. 2 *A*. In this figure, percent change of GABA inhibitory effect shows negative value, which means that GABA inhibitory effect decreased by penicillin application. This decreasing GABA inhibitory effect was still present 3 min after penicillin cessation.

3. *Post-discharge inhibition.* — Suprathreshold stimulation through an electrode placed on the surface of the hippocampus produced a discharge of the pyramidal cells followed by inhibition. The arrest of firing lasted 50-150 msec (Fig. 3 right side, inserted figure).

The duration of this inhibition was analyzed before, during, and following penicillin iontophoresis (Fig. 3). In 10 of the 15 cells tested the duration of inhibition was progressively shortened to 30-70 msec during the first 3 min of penicillin iontophoresis. Duration of the inhibition fluctuated in 2 cells, and did not change in 3 cells. After the cessation of penicillin iontophoresis the inhibition was usually longer and more variable than during the control period.

II. *Olfactory Bulb.*

The activity of 68 extracellular olfactory bulb cells was recorded in 22 cats. Fifty five of 68 were physiologically identified as mitral cells. The remaining 13 cells which were considered as non-mitral cells had longer latency or followed only lower rate (less than 30/sec) of electrical stimulation. The following findings are described for 55 mitral cells only.

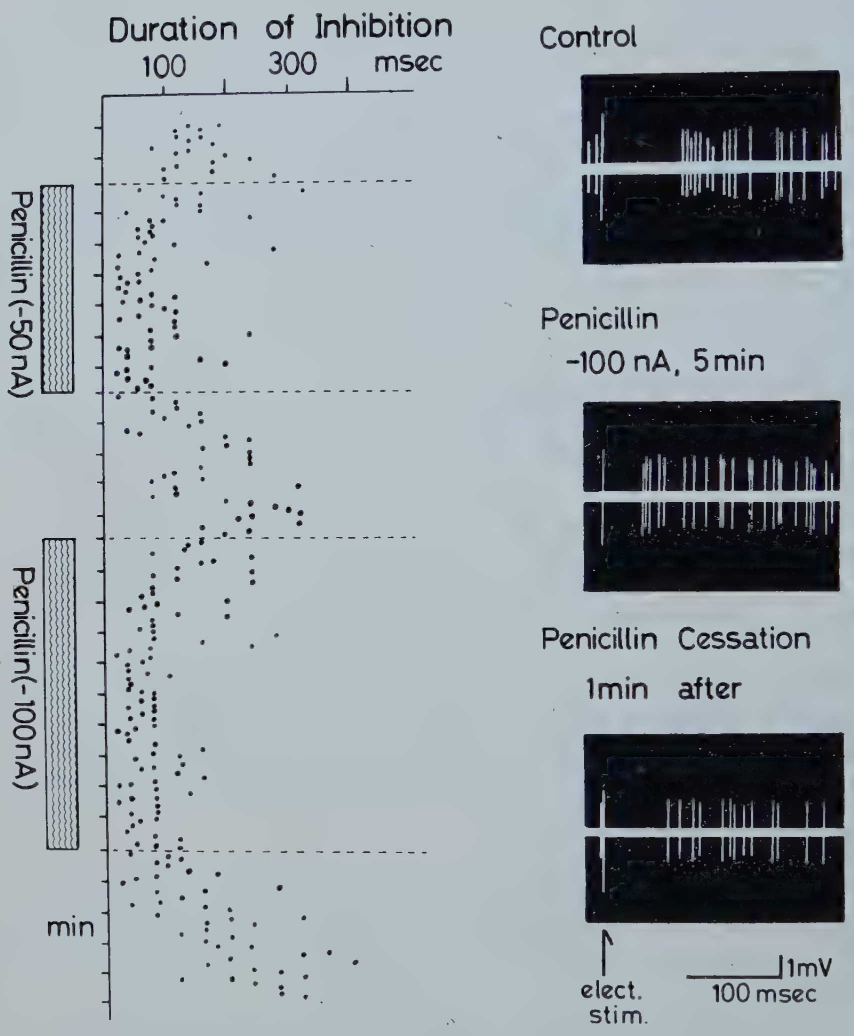

Fig. 3. – *Effects of penicillin on post-discharge inhibition* (*hippocampus*).

Example of changes in the duration of post-discharge inhibition of a pyramidal cell during penicillin iontophoresis are presented. Right side: Electrical stimulation produced a post-discharge inhibition of 50-150 msec duration (Control). After 5 min of penicillin iontophoresis (– 100 nA) the duration of inhibition was shortened. After 1 min cessation of penicillin duration of inhibition prolonged again. Left side: The effect of penicillin (– 50 nA, – 100 nA) on the duration of post-discharge inhibition is demonstrated in time course.

The amplitude of the spikes ranged from 0.2 to 7.0 mV, and the frequency of the spontaneous discharge was usually 5-20 c/sec. Fifty-one of 55 cells increased their firing rate with – 1 to – 10 nA current of DLH iontophoresis.

1. *Firing rate.* — Penicillin was applied iontophoretically for 10.5 min and the change in the firing rate was examined in 14 cells. Application of – 50 nA pe-

nicillin produced increase of firing rate in 12 cells (85.7%) and decrease in 1 cell. The other cell showed fluctuation of firing rate during penicillin application. Average increasing during penicillin application in the 12 cells was 135.6% of control firing rate. In 4 cells neither burst (cluster) of firing nor surface interictal discharge was noted even for 30 to 60 min penicillin iontophoresis.

2. *GABA effects.* — *a*) Continuous GABA iontophoresis: GABA was applied continuously (2-13 nA) to 5 cells and the effect of penicillin on the inhibitory response to GABA was examined. GABA initially suppressed unit firing almost completely. However, 1-5 min after the onset of penicillin iontophoresis the unit firing reappeared and gradually increased in frequency in 4 of 5 cells. In 1 cell GABA (13 nA) suppressed unit firing completely before and during penicillin iontophoresis.

b) Intermittent GABA iontophoresis: GABA was applied intermittently to 15 cells during continuous penicillin iontophoresis. The GABA inhibitory effect was evaluated by the same procedure as described before in the section of hippocampus. The GABA inhibitory effect was decreased during penicillin iontophoresis in 12 of these 15 cells. This decrease of GABA inhibitory effect was 28.4% (mean value for 12 cells during penicillin application). In the remainder 3 cells, 1 showed no change of GABA inhibitory effect during penicillin application, 1 fluctuated and 1 showed increase of GABA effect.

3. *Post-discharge inhibition.* — Single shock to the lateral olfactory tract produced arrest of mitral cell firing for 30 to 100 msec. This duration, which was directly related to the strength of stimulation, was examined before, during, and following penicillin iontophoresis in 10 cells. Single shock stimulation was applied in 3 to 4 sec intervals to the olfactory tract and strength of the stimulation was adjusted to produce a 80-100 msec pause of firing.

In 7 of the 10 cells a shortening of the duration was noted during penicillin application. The duration was prolonged in 2 and did not change in 1 cell during penicillin application.

EFFECTS OF PENICILLIN TOPICAL APPLICATION ON A SINGLE CELL.

I. *Hippocampus.*

Extracellular recordings of 64 pyramidal cells from the hippocampus were considered suitable for analysis. Resting surface activity from the hippocampus usually exhibited a regular 5-12 c/sec rhythm between 50 and 300 μV amplitude, mixed with small amplitude fast (15-30 c/sec) and slow (2-3 c/sec) activities.

Within 6 min after topical penicillin application 300-500 μV surface paroxismal discharges began to appear. These were predominantly monophasic transients which rapidly increased in amplitude (1-2 mV) and in complexity of form. The initial sporadic occurrence of the surface interictal discharges gradually became more regular over 5 to 15 min and developed a more stereotyped form. The following stages based on the patterns of surface activity, were defined after topical penicillin application for further examination (Fig. 4 *A*). Stage (*a*): time from the moment of topical penicillin application to the minute prior to the first interictal discharge. Stage (*b*): the minute preceding the first interictal discharge. Stage (*c*): time from the first interictal discharge to the minute proceding the first ictal episode. Stage (*d*): the minute preceding the first ictal event. Stage (*e*): time during each ictal episode, and Stage (*f*): time during all interictal episodes following the first ictus.

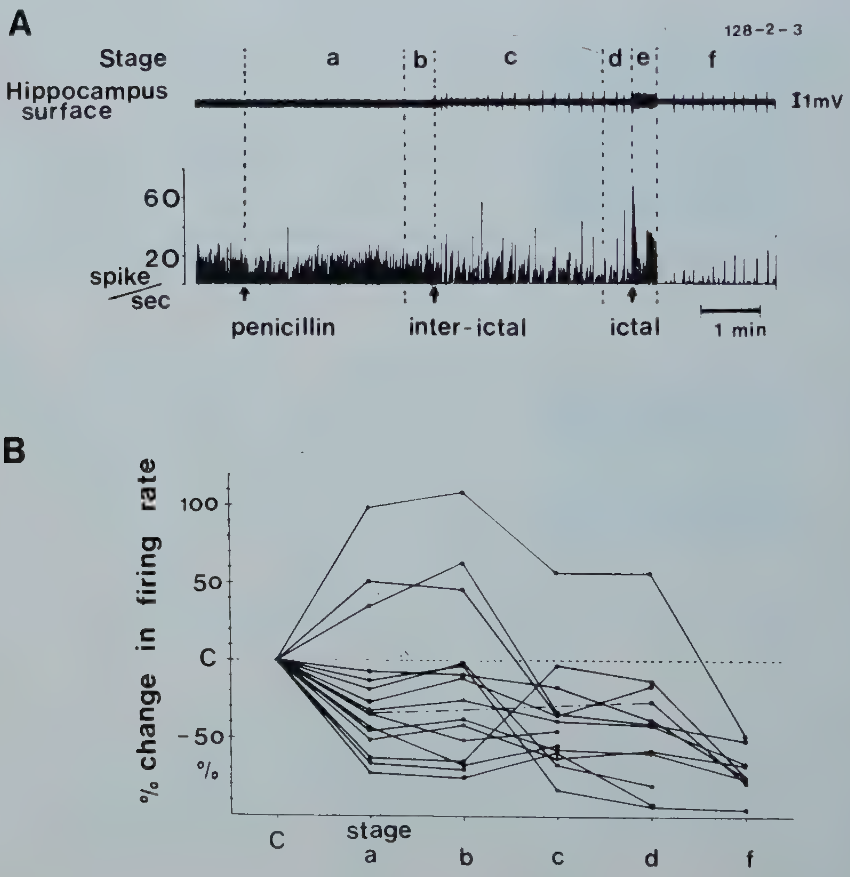

Fig. 4. – *Changes in the firing rates before and after topical penicillin application (hippocampus).*

A: Both the hippocampus surface activity and the unit firing rate changes are presented simultaneously. After the topical penicillin application (penicillin), the first interictal paroxysmal discharge was observed from the surface record (interictal). These paroxysmal discharges rapidly increased in amplitude becoming more regular and stereotyped in form. Stage (*a*) through (*f*) represent the different stages as described in text.

Changes in the firing rates are presented as a rate meter analysis. Firing rates are not increased either prior to the first interictal or ictal events.

B: Changes in the firing rates at the various stages based on the patterns of the surface activity (see *A*, upper) are presented from the 16 cells analyzed.

1. *Firing rates.* — The mean firing rate in 1 min was calculated at each stage and compared with the control (before penicillin topical application) mean firing rate.

The following changes in firing rates were noted at the various stages (Fig. 4 *B*). Stage (*a*): in 13 of 16 cells, after topical penicillin application the unit firing rate declined between 7.2% and 73% of the control rate; in 3 cells the increase exceeded the control firing rate. Stage (*b*): during the minute prior to the first surface interictal discharge, the unit firing rates were higher than at stage (*a*) in 8 cells, and lower than stage (*a*) in 7 of 16 cells; in 1 cell an ictal event occurred without an identifiable interictal stage. Stage (*c*): after the first surface interictal discharge the unit firing pattern changed with the spikes tending to fire in clusters, corresponding to the surface interictal discharge; after each of such cluster, the firing was suppressed between 200-1500 msec; the groups of spikes gradually became more regular in occurrence and the post-discharge suppression became longer in duration the higher the incidence of the interictal discharges; however, the unit firing rate remained below that of the control level in 13 of 14 cells, and was less than stage (*b*) in 10 of 14 cells. Stage (*d*): Unit firing rates during the minute preceding the ictal events were lower than the control level in 11 of 12 cells, and lower than in stage (*c*) in 8 cells. Stage (*f*): the average back-ground firing rate was calculated from the sum of unit spikes between 2 min and 10 min (or untile the next ictal episode, if less than 10 min). The average firing rate during stage (*f*) was less than during stage (*c*). The unit firing pattern became progressively more organized into regular clusters of spikes, corresponding to the surface interictal discharges. Post-interictal discharge periods were usually associated with a prolonged absence of unit firing.

2. *GABA effects.* — GABA was continuously applied for long periods either prior to, or shortly after topical penicillin application in 5 cells. Initially, GABA completely suppressed unit firing, but during the 18-80 sec prior to the first interictal discharge the GABA suppression was incomplete (see Fig. 5 *A* lower). In stage (*c*), the clusters of spikes associated with surface interictal discharge were not affected by GABA; the unit spikes not associated with surface interictal discharges on the other hand were markedly suppressed by GABA.

Intermittent GABA application at 30-90 sec interval was performed on 17 trials (N = 8 cells). Intermittent GABA application suppressed unit activity in the intervals between, but not during the interictal discharges (Fig. 5 *B*), as with continuous GABA application.

3. *Post-discharge inhibition.* — Using suprathreshold stimulation of the alveus or fimbria the duration of inhibition was analyzed before and after topical penicillin application in 14 cells (Fig. 6). Duration of such post-discharge inhibition was slightly longer during the first 1-2 min after topical penicillin application than before application; then it returned to the control range. The duration of post-discharge inhibition was not significantly different either before or after the

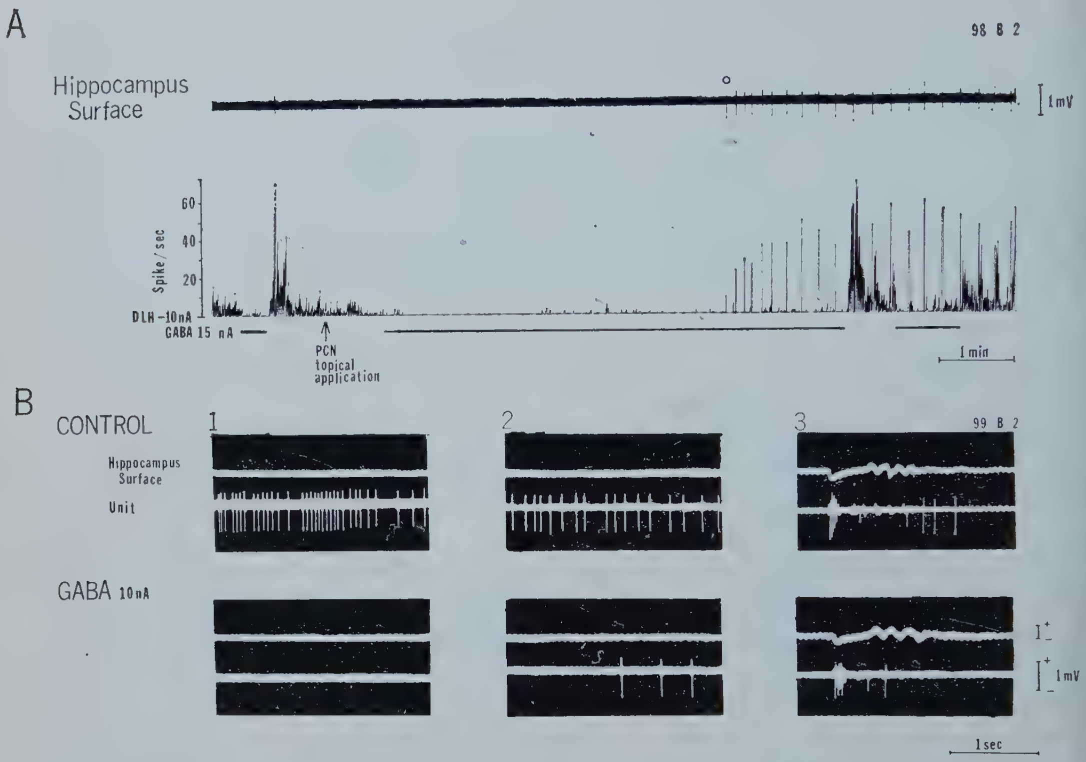

Fig. 5. – *GABA effects on the cell with topically applied penicillin* (*hippocampus*).

A: Hippocampus surface activity (top), and firing rate by rate meter analysis (bottom) are presented simultaneously. DLH (– 10 nA) activated unit firing was almost completely suppressed by GABA (15 nA) before topical penicillin application. GABA could also generally suppress the firing after penicillin topical application except for only a few unit discharges observed before the occurrence of the first interictal paroxysmal discharge. The clusters of spikes associated with surface interictal discharges were not affected by GABA.

B: The effect of GABA on unit discharges (lower row of figures) are shown compared to the control firing (upper row of figures in each stage: 1) before topical penicillin application, 2) 30 seconds prior to first interictal discharge and 3) during an interictal paroxysmal discharge. The clusters of spikes associated with surface interictal discharges are almost completely unaffected by GABA (see 3 of the figure).

onset of the surface interictal discharges. However, after an ictal discharge, the unit firing rate became so infrequent that the duration of post-discharge inhibition was difficult to evaluate.

II. *Olfactory Bulb.*

Mitral cell potential was recorded from the olfactory bulb extracellularly and identified electrophysiologically. Thirty-two extracellular units were considered suitable for anaysis of this study. The amplitude of the spikes ranged from 0.5 to 6 mV. Since spontaneous firing rate usually exceeded 10 spikes/sec in most cells,

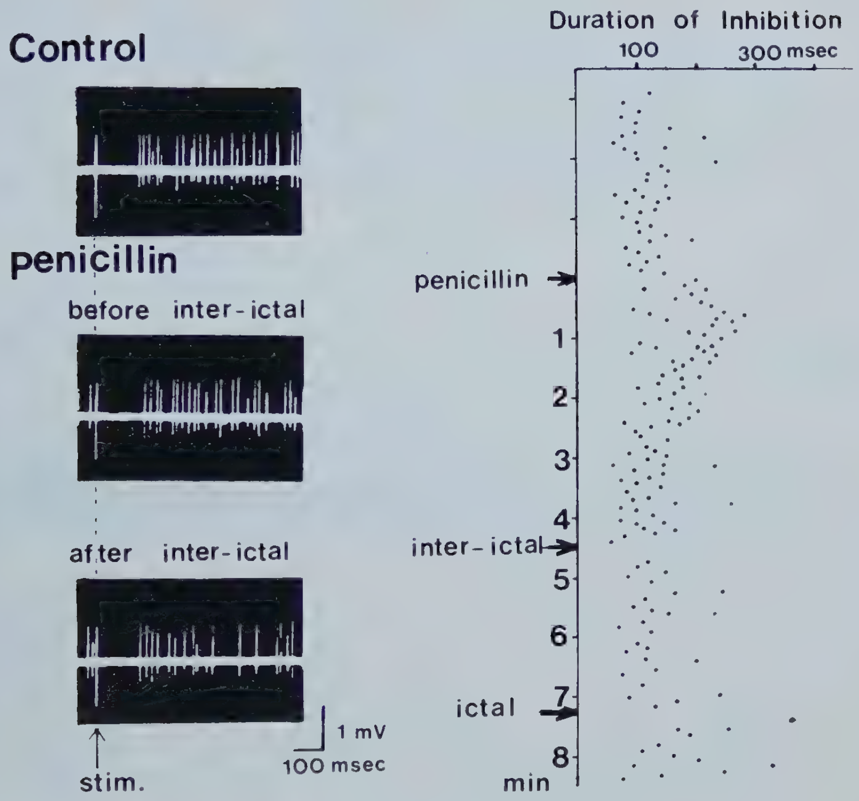

Fig. 6. – *Changes in post-discharge inhibition (hippocampus).*

An example of changes in duration of inhibition following topical penicillin application is presented. During a succession of electrical stimulations of the hippocampus surface, penicillin was topically applied. Post-discharge inhibition produced by electrical stimulation was slightly longer than the control. Thereafter, no significant differences in duration are noted.

DLH applied to only a few cells for maintainance of firing rate at 10 spikes/sec or more.

Resting surface activity recording by bipolar surface electrodes from the olfactory bulb usually showed burst appearance of 15 to 25 c/sec fast activity with 3 c/sec to 8 c/sec wave.

1. *Firing rate.* — Changes in firing rate were examined on 12 cells before and after penicillin topical application to the olfactory bulb. The mean firing rate was calculated at each 30 sec period after penicillin topical application and compared with the control (before penicillin topical application) mean firing rate. Percent changes of the firing rate were expressed by the same formula as described in the section of hippocampus.

In the majority of cells (8 out of 12) firing rate transiently increased after penicillin topical application. After that, firing rate exceeded the control level again and continuously increased before reaching a plateau in 8 cells. The remainder 3 cells in this stage showed fluctuation of firing rate, and in one cell the firing rate was below the control level (Fig. 7).

The firing pattern showed no obvious changes even 60 min after penicillin topical application. The surface activity was not significantly changed and no epileptiform activity was observed from olfactory surface even after several hours (Fig. 7, upper).

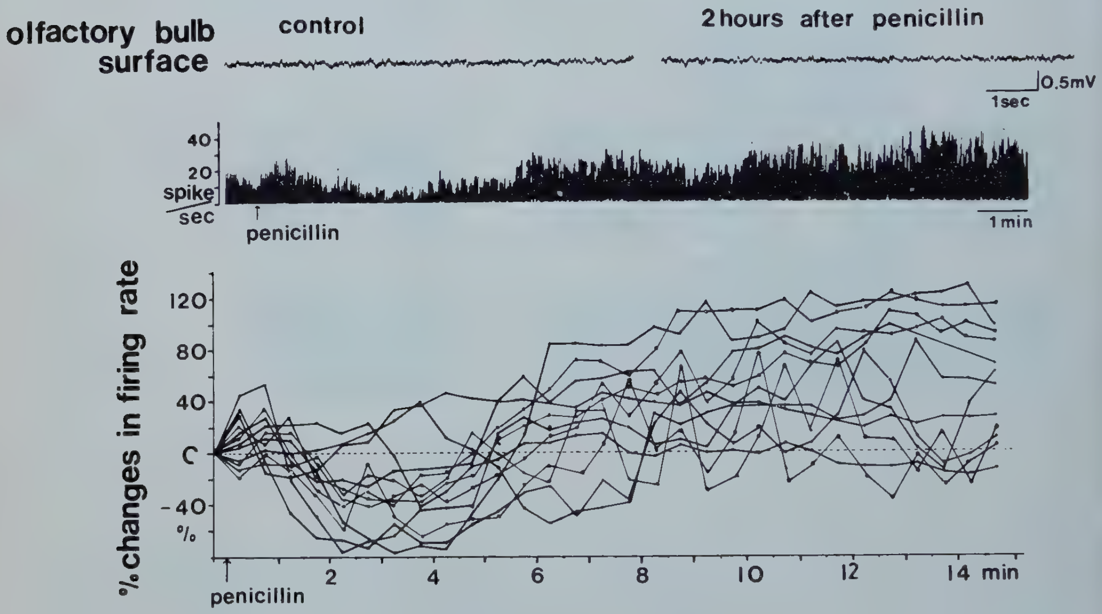

Fig. 7. – *Changes in the firing rates before and after topical penicillin application (olfactory bulb).*

Upper row: Olfactory bulb surface activity before and 2 hour after penicillin topical application. No obvious seizure activity is observed even 2 hours after penicillin application.

Middle row: An example of changes in firing rate before and after topical penicillin application. Changes in the firing rates are presented as a rate meter analysis.

Lower row: Changes in the firing rate are presented from the 12 cells analyzed.

2. *GABA effects.* — GABA was applied intermittently to 15 cells before and after penicillin topical application on the surface of olfactory bulb. 2-17 nA current was required for GABA to completely suppress the unit firing before penicillin topical application. However, after penicillin application, complete suppression of firing with these same doses of GABA either required a longer time or did not occur (Fig. 8 *A*).

In order to quantitatively evaluate the suppression effect of GABA, firing rate was calculated at every other minute and compared with the control (before penicillin application) firing rate as described in the section of hippocampus. The decrease of GABA inhibitory action was observed after about 5 minutes in most cells (Fig. 8 *B*).

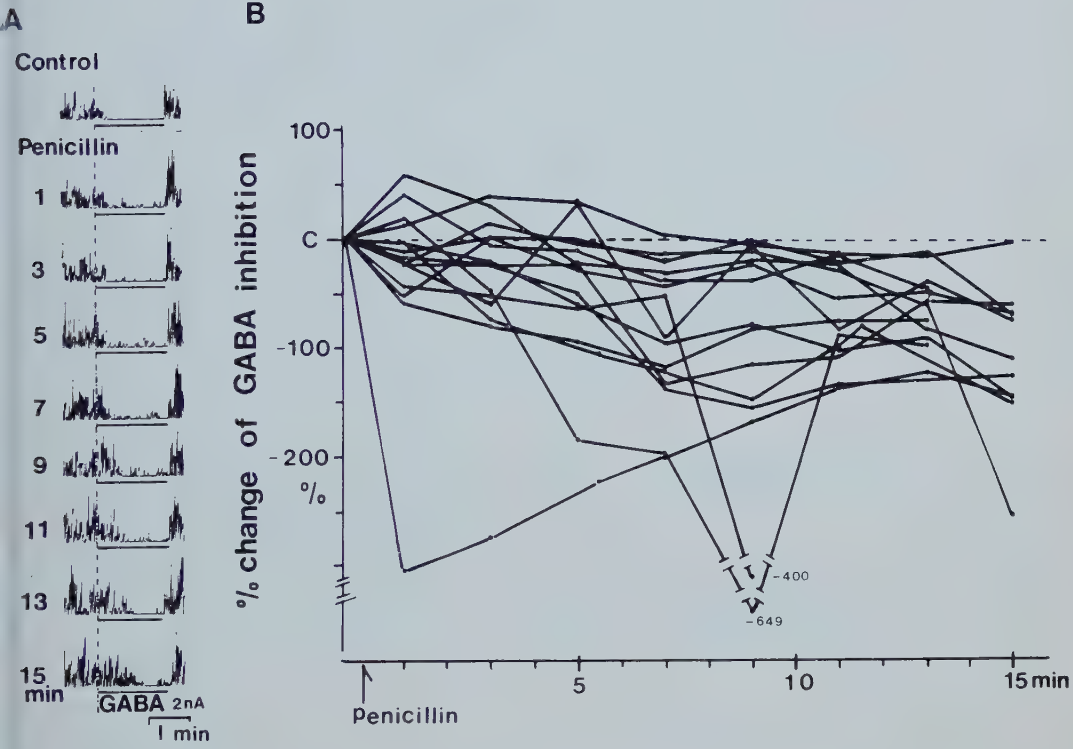

Fig. 8. – *GABA effects on the cell with topically applied penicillin (olfactory bulb).*

A: GABA was applied intermittently before and after penicillin topical application on the surface of olfactory bulb. An example of firing rate by rate meter analysis before (control) and 1, 3, 5, 7, 9, 11, 13 and 15 min after penicillin topical application. 2nA GABA completely suppresses firing in control. However, after penicillin application these same doses of GABA either required a longer time for complete suppression of firing or failed to completely suppress unit firing.

B: Percent change of GABA inhibitory action (see text for calculation method) of 15 cells are presented. The decrease of GABA inhibitory action (negative value) was observed in most cells.

3. *Post-discharge inhibition.* — Stimulation of lateral olfactory bulb through a surface electrode by suprathreshold (20-40V) electrical stimulation (0.1 msec, 0.2-0.3Hz) inhibited the firing discharge of the mitral cell for fifty up to several hundreds millisecond, depending on the current strength.

The changes in the duration of this inhibition were examined before and after penicillin application in 6 cells. Shortly after the penicillin topical application on the olfactory bulb surface, the duration of inhibition usually increased transiently and returned to control level within 2 or 3 min. After that it began to decrease significantly, compared with control in 4 cells, and did not change in 2 cells for 13 and 20 min after topical penicillin application (Fig. 9).

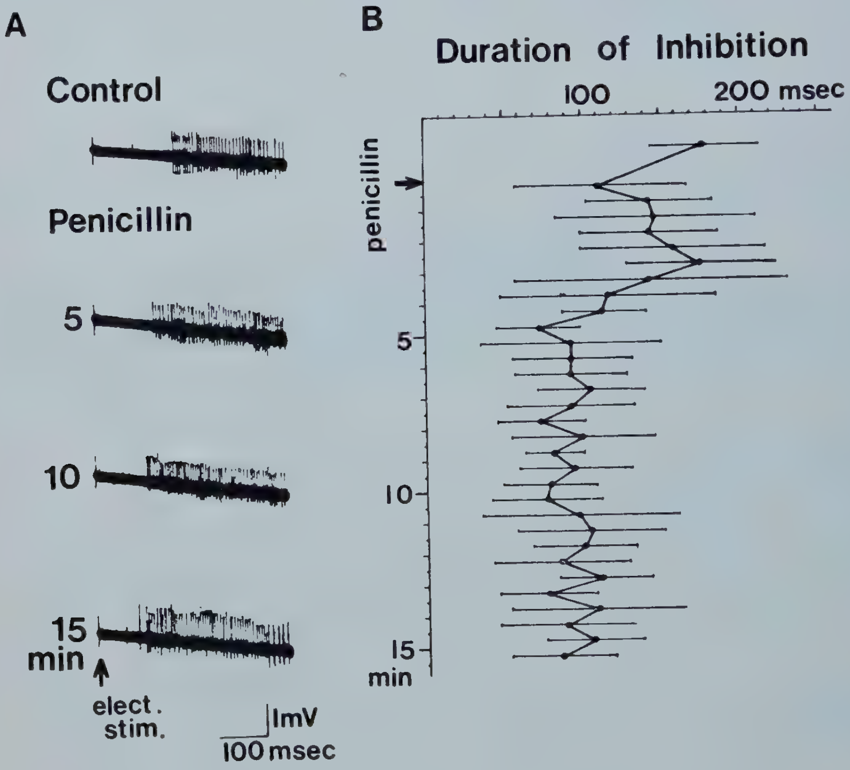

Fig. 9. – *Changes in post-discharge inhibition (olfactory bulb).*

An example of changes in duration of inhibition following topical penicillin application is presented. Electrical stimulation of the lateral olfactory tract produced post-discharge inhibition before penicillin topical application (control). After topical penicillin application on the olfactory bulb surface (5, 10 and 15 min after) this duration of inhibition shortened (*A*). Successive analyses of this duration of inhibition are presented by the mean value and standard error for 30 sec analysis (*B*).

DISCUSSION

Penicillin iontophoresis

1. *Changes in firing rate.* Penicllin iontophoresis has been reported to increase the firing rates of most cells in the feline cerebral cortex within 6-20 min after the onset of low dose (– 40 nA) drug application (23; see also 10). However, according to Davidoff (4) it did not affect the firing rate in the majority of spinal cord cells.

In the present investigation of hippocampus pyramidal cells, 94.2% of 52 spontaneous or DLH activated cells had increase firing rates during penicillin iontophoresis of – 20 to – 100 nA. Olfactory bulb mitral cells also showed the increasing of firing rate in 85.7% of cell by – 50 nA penicillin iontophoresis. As far as the effect of penicillin on firing rate of a single cell is concerned, there is no significant difference between hippocampus pyramidal cell and olfactory bulb mitral cell. This fact suggests that penicillin has an excitatory effect on both cells.

2. *Changes in GABA inhibitory effect.* After the first suggestion (9) that GABA might be involved in the control of neuronal excitability, the action of GABA in various parts of the nervous system has been investigated intensively. These investigations have shown a striking similarity with the effects of synaptic inhibition, *i.e.* in hippocampus (e.g., 1) and olfactory bulb (e.g., 15).

Penicillin has been reported to reduce GABA effects. In this study GABA inhibitory action on hippocampus pyramidal cell and also on olfactory bulb mitral cell was confirmed. GABA could suppress firing discharge and its action was reduced following penicillin iontophoretic application in the majority of both hippocampus pyramidal cells and olfactory bulb mitral cells. There were no significant difference between the two kinds of cells.

3. *Post-discharge inhibition.* A progressively shortened duration of the post-discharge inhibition during penicillin iontophoresis was compatible with a penicillin induced antagonism of GABA. This may reflect a decrease of GABA inhibitory action mediated via hippocampal basket cells or olfactory bulb granule cells, since GABA is presumed to be the inhibitory transmitter released by such cells (2, 15). These phenomena were observed both in hippocampal pyramidal cell and olfactory bulb mitral cell.

Topical application

Although similar results were obtained from penicillin iontophoresis studies on hippocampal pyramidal cell and olfactory bulb mitral cell, several different findings were observed from the study of penicillin topical application on hippocampus and olfactory bulb: Topical and iontophoretic penicillin application to the olfactory bulb mitral cell produced increasing firing rates, decreasing GABA inhibitory action and shortening of the post-discharge inhibition. On the other hand, in the case of the hippocampus, topical penicillin application and penicillin iontophoresis yielded significantly different results.

In the hippocampal cell, the unit firing rate was not increased immediately prior to the first interictal discharge (during stage (*b*)). This is consistent with intracellular data (14) indicating that there is not a gradual decrease in membrane potential before the sudden occurrence of the large PDS (which corresponds to the surface interictal discharge). However, this fact is in contrast to the finding that with penicillin iontophoresis the unit firing rate would increase and the GABA inhibitory action decrease.

There are several possible explanations for this apparent discrepancy. First, it is possible that, when applied to the cortical surface, penicillin does not reach the cell. Macon and King (13) have reported a similar lack of effect in the feline cortical neurons, indicating that this may be due to failure of the topically applied epileptogenic agent to penetrate 1-2 mm into the somatosensory cortex. Recent investigation suggests that the rate of topical penicillin diffusion into the feline cortex is 1.5 mm/h (16). Using the end point as induction of seizure activity in perfused guinea pig brain slices, Schwartzkroin and Prince (18) determined that concentration of penicillin as low as 1.7 m*M* may be effective. Davenport *et al.* (3) have calculated that the time required for this concentration of penicillin to penetrate to 1 mm depth was between 3.5 and 4.2 min, and to depth of 2 mm, between 14 and 17 min. Since the hippocampal pyramidal cells in the present study lie at the depth of 0.3 to 0.6 mm, and the penicillin concentration at the surface of hippocampus was higher than assumed by Davenport *et al.* in their model, the effective seizure producing concentration at the level of the hippocampal pyramidal cells might be expected to occur in less than 4.2 min. Furthermore, in the case of olfactory bulb, firing rate increased from 5 to 8 min after the topical penicillin application. This also suggests that penicillin will affect the cell either directly or indirectly within several minutes.

Next, there is the possibility that none of the cells which were sampled, but only the surrounding pyramidal cells were primarily affected by penicillin; that is, the cell under examination was only involved secondarily. We can not completely exclude this possibility, because a microelectrode recording is a sampling study from many cells. However, our results are consistent with the previous reports (13, 14). The chance that all the surrounding cells are influenced by penicillin, and that only the cell under examination is unaffected appears unlikely.

Another possible explanation for the lack of changes after topical penicillin application to the hippocampus pyramidal cells is that the cells may have different sensitivities to penicillin even in the same neuronal structures, as demonstrated in the spinal cord (3), and in the hippocampus where Schwartzkroin and Prince (19) have shown regional differences to the epileptogenic action of penicillin in the hippocampal pyramidal cells: The CA3 cells always seemed to precede the CA1 cells in the formation of bursts after hippocampal slices were placed into a penicillin bath. The CA1 pyramidal cells in a normal medium were not significantly different in resting membrane potential, resistance and time constant from the cells rendered epileptogenic in the penicillin bath. However, interictal and/or ictal events occurred consistently following penicillin topical application to a restricted CA1 region in this study, and no apparent difference in results from the neurons in the CA1 and CA3 areas were observed.

Another possible explanation is based on our results of topical penicillin application on the olfactory bulb, in which firing rate increased several minutes after the application without generating surface epileptiform activity. In the hippocampus, the appearance of surface epileptiform activity may obscure observation of the changes in pyramidal cell firing rate. Since the epileptic phenomenon is a pathophysiological event characterized by excessive synaptic bombardment, ephaptic conduction, and/or antidromic backfiring (8, 17), normal neuronal functions may be disturbed and masked by severe epileptic storm. This is why in the olfactory bulb, in the absence of epileptiform activity, changes in firing rate, GABA inhibitory effect and post-discharge inhibition could be clearly observed and these were similar to the iontophoresis data. On the other hand, in the hippocampus epileptiform activity masked changes in firing rate, GABA inhibitory action and post-discharge inhibition, because epileptiform activity occurred before pyramidal cells were directly affected by penicillin.

If this assumption is accepted, the questions arise as to where and how epileptic discharges occurred in the hippocampus and why epileptiform activity is not generated in the olfactory bulb. We do not have an answer to these questions. We only suggest the possibility that cells might have different sensitivities to the effect of penicillin: e.g. small cells may have a higher sensitivity than large (pyramidal) cells. Therefore, the primary effect of topical penicillin may occur at the small cells and/or interneurons. Subsequent epileptiform activity may be produced through the activation of these small cells, with secondary involvement of the pyramidal cell in the early stages. At later stages, strong epileptiform discharges obscure possible changes in the function of pyramidal cells.

Mechanisms in the generation of epileptiform discharges.

Long duration iontophoretic application of penicillin presumably to a single cell or to a restricted cell population only produced an increased firing rate without any observable surface paroxysmal discharge. In the case in which penicillin leaked from a broken electrode, the surface interictal activity was noted to occur with a corresponding abrupt change in the unit firing pattern (from random individual spiking to clusters of spikes) and subsequent long-lasting post-discharge silent periods. This process lacked a continuity of change in firing. These findings support the proposed mechanism of epileptogenesis requiring the activation of a minimal cell population.

Enhancement of " positive feedback system " or " recurrent excitation " have been considered to play a role in the generation of epileptic activity in hippocampus (12) and in neocortex (21). On the other hand, the failure to develop paroxysmal discharges is predicted by the lack of a recurrent excitatory system in cerebellar cortex (6). The special disynaptic dendro-dendritic type recurrent inhibition, and the long latency recurrent excitatory synchronous discharges (15) present in the olfactory bulb might have some bearing in preventing the generation of epileptic activity in the structure. These synaptological mechanisms are helpful to explain the different potency of an epileptogenic agent in different neuronal structures. However, small cells (which are hard to investigate even by microelectrode) and glial cells (idle cells) may also play an important role in determining the different threshold for epileptogenic activity (5).

SUMMARY

This investigation was carried out to clarify the mechanisms for production of different seizure threshold. To study this problem changes of a single cell activity were examined by means of penicillin iontophoretical application to a single cell of both low seizure threshold hippocampus and the high seizure threshold olfactory bulb, and also topical application to the surface of hippocampus and olfactory bulb.

1. Penicillin was applied iontophoretically using five barrel glass micropipettes. Extracellular recordings from 58 hippocampal pyramidal cells and 68 olfactory bulb mitral cells were analyzed.

Penicillin increased the firing rate in most of both hippocampal pyramidal and olfactory bulb mitral cells. This suggests that penicillin finally had an excitatory effect on both cells. The results from the experiments of intermittent and continuous GABA application on a cell during penicillin iontophoresis revealed that GABA inhibitory action was reduced by penicillin in both cells. A progressively shortend duration of the post-discharge inhibition during penicillin iontophoresis also suggested that penicillin may reflect a decrease of GABA inhibitory action. No obvious seizure activity and/or no change of firing pattern were observed even after long penicillin iontophoresis. There was no significant different responses to penicillin iontophoresis in the hippocampus and the olfactory bulb single cell.

2. Extracellular activity from 64 hippocampal pyramidal cells and 32 olfactory bulb mitral cells was recorded. The effects of penicillin topical application on single cell function were examined.

From hippocampus surface, paroxysmal activity begun to appear within 6 min after topical application, and became more regular and stereotyped in form. The firing rate initially decreased in the majority of cells, with no increase prior to interictal or ictal events. The unit responses to both intermittent and continuous GABA iontophoresis was suppression in unit firing incidence, except for the burst patterns associated with the surface interictal or ictal discharges. Post-discharge inhibition was not significantly different either before or after the onset of the surface interictal discharges. These results indicate the firing rate and inhibitory function of the hippocampal pyramidal cells were not significantly changed during and following the development of interictal and/or ictal epileptiform activity.

Olfactory bulb surface activity was not significantly changed and no epileptiform activity was observed even several hours after topical penicillin application. Changes in firing rate exhibited exceeding the control level in the majority of cells 5-8 min after penicillin application. GABA inhibitory action decreased by penicillin topical application after about 5 min in most cells. The duration of inhibition of mitral cell firing which was produced by lateral olfactory tract electrical stimulation decreased significantly after penicillin application.

To summarize, topical and iontophoretic penicillin application showed similar results in the olfactory bulb without generating surface seizure discharges. However,

with topical penicillin application to the hippocampus there was no significant change of unit function.

The present results suggest that single cell itself may not have different properties to generate either epileptic activity or difference of seizure threshold, and a critical population of directly activated cells may be required to generate seizure activity. The mode of synaptic connection may play an important role in determining the different threshold for epileptogenic activity.

Acknowledgements. — The authors wish to thank Mr. S. Walbridge and Miss. J. Ling for technical assistance.

REFERENCES

1. Biscoe, T. J., and Straughan, D. W. The pharmacology of hippocampal neurons. *J. Pharmacol.*, **17**: 60-61, 1965.
2. Curtis, D. R., Felex, D. and McLennan, H. GABA and hippocampal inhibition. *Brit. J. Pharmacol.*, **40**: 881-883, 1970.
3. Davenport, J., Schwindt P. C. and Crill, W. E. Penicillin-induced spinal seizures: Selective effects on synaptic transmission. *Exp. Neurol.*, **56**: 132-150, 1977.
4. Davidoff, R. A. Penicillin and presynaptic inhibition in the amphibian spinal cord. *Brain Res.*, **36**: 218-222, 1972.
5. Dichter, M. A., Herman, C. J. and Selzer, M. Silent cells during interictal discharges and seizures in hippocampal penicillin foci. Evidence for the role of extracellular K^+ in the transition from the interictal state to seizures. *Brain Res.*, **48**: 173-183, 1972.
6. Eccles, J. C. Ito, M. and Szentagothai, J. *The Cerebellum as a Neuronal Machine*. Berlin, Springer, 1967.
7. Green, J. D., Mancia, M. and von Baumgarten, R. Recurrent inhibition in the olfactory bulb. I. Effects of antidromic stimulation of the lateral olfactory tract. *J. Neurophysiol.*, **25**: 467-488, 1962.
8. Gutnick, M, J. and Prince, D. A. Thalamocortical relay neurons: antidromic invasion of spikes from a cortical epileptogenic focus. *Science*, **176**: 424-426, 1972.
9. Hayashi, T. Effects of sodium glutamate on the nervous system. *Keio J. Med.*, **3**: 183-192, 1954.
10. Hill R. G., Simmonds, M. A. and Straughan, D. W. A comparative study of some convulsant substances as GABA antagonists in the feline cerebral cortex. *Br. J. Pharmac.*, **49**: 37-51, 1973.
11. Kandel, E. R., Spencer, W. A. and Brinely, F. T. Jr. Electrophysiology of hippocampal neurons. I. Sequential invasion and synaptic organization. *J. Neurophysiol.*, **21**: 225-242, 1961.
12. Lebovitz, R. Dichter, M. and Spencer, W. A. Recurrent excitation in hippocampus. *Fed. Proc.*, **28**: 455, 1969.
13. Macon, J. M. and King, D. W. Penicillin iontophoresis and the responses of somatosensory cortical neurons to amino acids. *Electroenceph. clin. Neurophysiol.*, **47**: 52-63, 1979.
14. Matsumoto, H. and Ajmone Marsan, C. Cortical cellular phenomena in experimental epilepsy: Interictal manifestations. *Exp. Neurol.*, **9**: 286-304, 1964.
15. Nicoll, R. A. Pharmacological evidence for GABA as the transmitter in the olfactory bulb. *Brain Res.*, **35**: 137-149, 1971.

16. PEDLEY, T. A. and NOEBELS J. L. Anatomical localization of 14C-penicillin in experimental focal epilepsy. *Neurosci. Abstr.*, **2**: 253, 1976.
17. SCHWARTZKROIN, P. A., MUTANI, R. and PRINCE, D. A. Orthodromic and antidromic effects of a cortical epileptiform focus on ventrolateral nucleus of the cat. *J. Neurophysiol.*, **38**: 795-811, 1975.
18. SCHWARTZKROIN, P. A. and PRINCE, D. A. Penicillin-induced activity in hippocampus slices maintained in vitro. *Neurosci. Abstr.*, **2**: 266, 1976.
19. SCHWARTZKROIN, P. A. and PRINCE, D. A. Cellular and field potential properties of epileptogenic hippocampal slices. *Brain Res.*, **147**: 117-130, 1978.
20. SMITH B. M. and HOFFER, B. J. A gated, high voltage iontophoresis system with accurate current monitoring. *Electroenceph. clin. Neurophysiol.*, **44**: 398-402, 1978.
21. TAKAHASHI, K., KUBOTA, K. and UNO, M. Recurrent facilitation in cat pyramidal tract cells. *J. Neurophysiol.*, **30**: 22-34, 1967.
22. VON EULER, C., GREEN, J. D. and RICCI, G. The role of hippocampal dendrites in evoked responses and after-discharges. *Acta physiol. scand.*, **42**: 87-111, 1958.
23. WALSH, G. O. Penicillin iontophoresis in neocortex of cat: Effects on the spontaneous and induced activity of single neurons. *Epilepsia*, **12**: 1-12, 1971.

Archives Italiennes de Biologie, 122: 301-309, 1984.

PROJECTIONS FROM THE CORTEX OF THE SUPERIOR TEMPORAL SULCUS TO THE DORSAL LATERAL GENICULATE AND PREGENICULATE NUCLEI IN THE MACAQUE MONKEY

M. G. MAIOLI, C. GALLETTI[1], S. SQUATRITO,
P. P. BATTAGLINI AND E. RIVA SANSEVERINO

Istituto di Fisiologia umana, Facoltà di Medicina
and Cattedra di Fisiologia generale, Facoltà di Farmacia[1], *Università di Bologna,*
Piazza di Porta S. Donato 2, 40127 Bologna, Italy

INTRODUCTION

On the basis of recent anatomical (20) and electrophysiological (2) investigations, the cortex of the superior temporal sulcus (STs) in the macaque monkey has been indicated as a multisensory field which includes unimodal as well as polymodal association areas (see Fig. 1 *A*). In particular, the caudal third of the STs is specifically correlated with the visual modality (27), so that is usually indicated as the visual region of the superior temporal sulcus. This cortical region, in turn, has been recently divided in various areas on the basis of electrophysiological and anatomical criteria (26). The best known of these areas is the middle temporal area (MT), lying in the floor and the deepest part of the lower bank of the STs and characterized by its heavy myelination (26) and its high incidence of neurons showing selectivity for direction and speed of motion of visual stimuli (17). This direction sensitivity also seems to be a feature of the neurons of the cortex adjacent to the MT, in the floor and the upper bank of the STs (26), so that the majority of the STs visual region may be concerned with the analysis of moving stimuli.

The aim of the present study has been to assess whether the different parts of the STs visual region are connected with one of the main subcortical stations of the visual system, that is to say the lateral geniculate body (LGb). The LGb consists of at least two anatomo-functional subdivisions: *i*) the dorsal lateral geniculate nucleus (DLGn), and *ii*) a portion indicated as the pregeniculate nucleus (PGn) in primates and the ventral lateral geniculate nucleus in other mammals (18). It is well known that both the DLGn and the PGn receive direct inputs from the retina (11, 19), the superior colliculus (1), and cortical visual areas (7, 8, 12, 22). As regards the STs cortex in the macaque monkey, while LGb afferents from the MT have recently been investigated (16, 25), possible projections from areas near the MT to the lateral geniculate body have yet to be delineated. The present work shows that the part of the visual cortical region adjacent to the MT is connected with both subdivisions of the LGb, whereas the MT itself, as well as the superior temporal polysensory region, projects into the PGn only.

METHODS

The experiments were carried out on 5 juvenile macaque monkeys (*Macaca fascicularis*). Under deep Nembutal anesthesia, each animal received 2 to 3 unilateral intracortical injections of a mixture of L-[5-^{3}H] proline and L-[4,5-^{3}H]leucine [90 μCi/μl; 0.8-1.0 μl/injection] deep in the cortex of the STs. After a survival period of 7 days, the animals were deeply reanesthetized and perfused with saline and a buffered solution of 10% formalin at 38° C.

Paraffin-included brains were coronally sectioned at 8-10 μm. One section out of every five was processed for autoradiography with a liquid emulsion (Kodak NTB-2) procedure and stained for cells with toluidine blue or cresyl-violet. Through the injection sites, sections adjacent to those autoradiographically treated were stained for fibers using a modified Heidenhain-Woelke method (see Ref. 6), in order to outline the limits of the MT (see Ref. 15). Serial sections of both hemispheres were observed by both bright- and dark-field microscopy and reproduced by camera lucida drawings. Criteria in delimiting the injection sites as well as further technical details have been reported in a previous paper (23).

RESULTS

As shown in Fig. 1 *B*, a number of radiolabeled aminoacid injections were performed in the banks and floor of the caudal half of the STs of different animals.

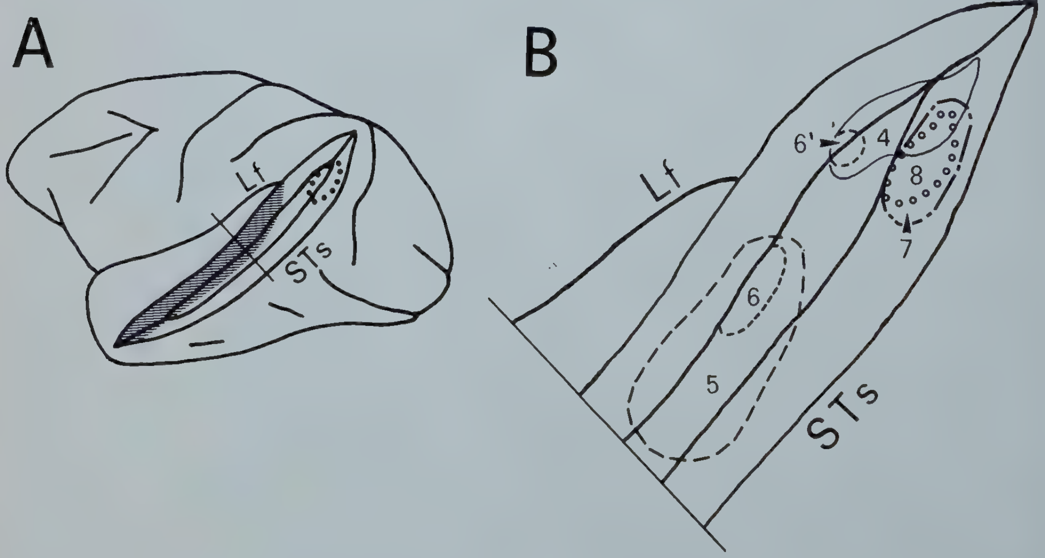

Fig. 1. – *Reconstruction of the injection sites of five different cases.*

A: Lateral view of the macaque brain with the superior temporal sulcus (STs) opened to show the outline of the middle temporal area (dots) and the superior temporal polysensory area (shaded region: according to Bruce *et al.* 2).

B: Increased extract of the caudal half of the open STs, on which are reported the injection sites of the different cases. Note that Case-6 is reported with two foci of injections (6 and 6′).

Abbreviations: Lf, lateral (sylvian) fissure; STs, superior temporal sulcus.

In all cases a bundle of corticofugal labeled fibers could be traced through the optic radiation and the internal capsule, posterior to the putamen, as far as the ipsilateral LGb. No label was found in the contralateral LGb.

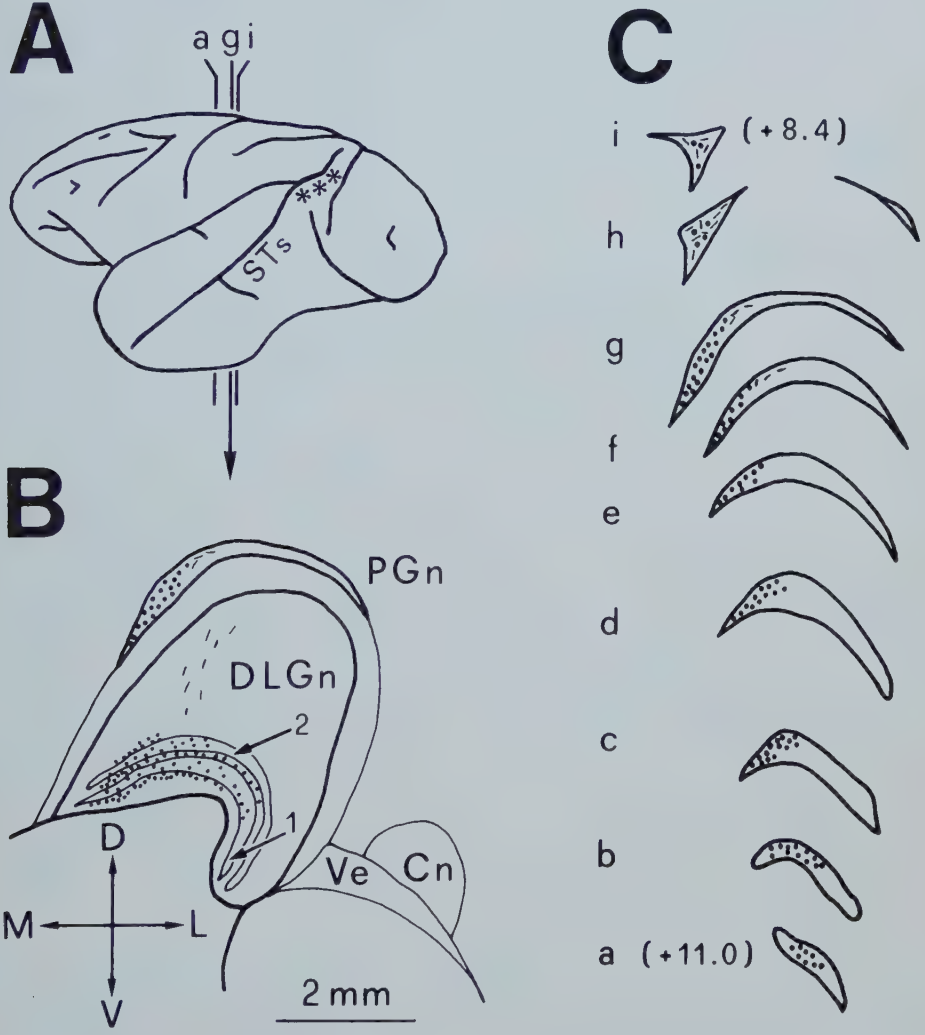

Fig. 2. – *Projections from the posterior part of the caudal half of the superior temporal sulcus to the pregeniculate and dorsal lateral geniculate nuclei* (*Case-4*).

A: Lateral view of the monkey's left hemisphere on which are indicated three frontal planes (*a*, *g*, *i*) out of those shown in the camera lucida reconstructions of *B* and *C*. The asterisks on the prelunate gyrus mark the extent of the injection site hidden in the banks of the superior temporal sulcus.

B: Camera lucida drawing of the lateral geniculate body at the level of section *g*. Only the magnocellular layers (laminae 1 and 2) of the dorsal lateral geniculate nucleus are outlined, to illustrate the pattern of silver grain distribution in the laminar and interlaminar zones.

C: Reconstruction of the pregeniculate nucleus. The stereotaxic planes are indicated near the rostral-most (*a*) and the caudal-most (*i*) frontal sections of the nucleus.

Abbreviations: Cn, caudate nucleus; DLGn, dorsal lateral geniculate nucleus; PGn, pregeniculate nucleus; STs, superior temporal sulcus; Ve, lateral ventricle; D, dorsal; V, ventral; M, medial; L, lateral.

The injection site of Case 4 (see Fig. 1 *B*) was at the caudal-most part of the STs and included a part of its lower bank, the fundus and a narrow strip of the upper bank of the sulcus. Fig. 2 illustrates the results of this case. The PGn was labeled, with silver grains accumulating in its medial and dorsomedial parts (Fig. 2 *B* and *C*, *a-g*). In the posterior-most sections (Fig. 2 *C*, *h*, *i*), labeled material was also observed to fill a region of the PGn which extended medially towards the zona

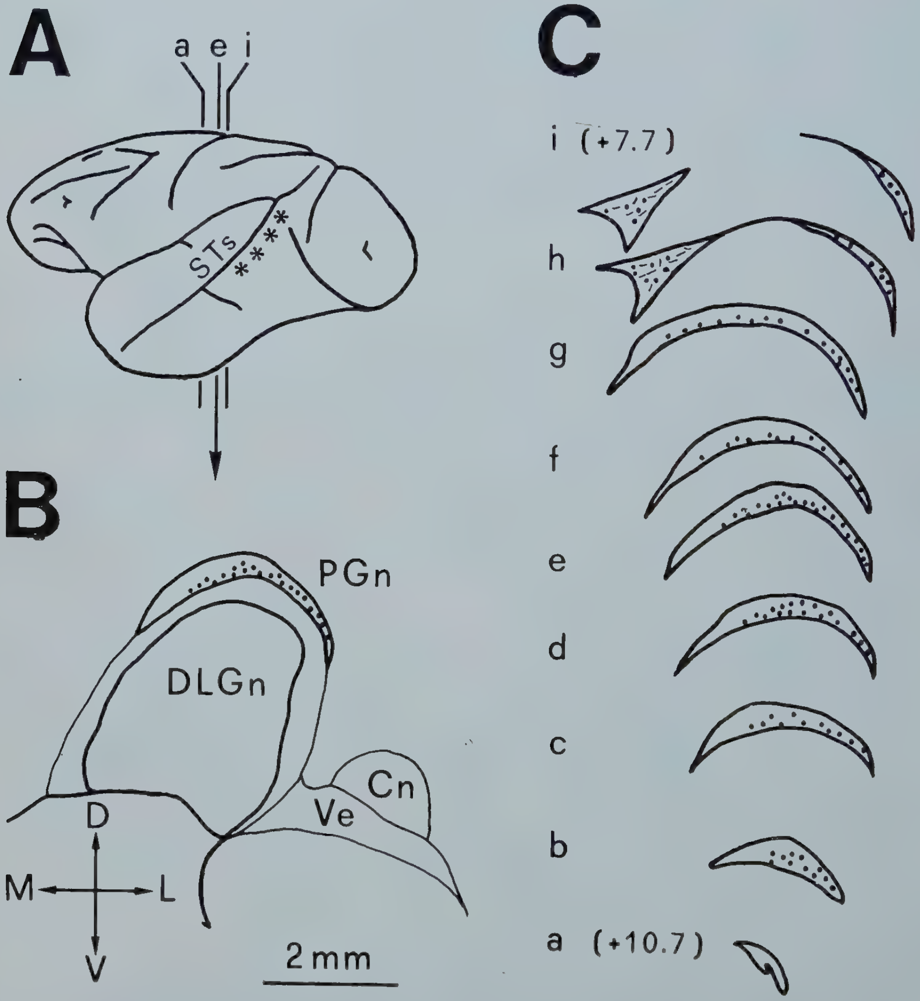

Fig. 3. – *Projection from the anterior part of the caudal half of the superior temporal sulcus to the pregeniculate nucleus (Case-5).*

A: Lateral view of the monkey's left hemisphere on which are indicated three frontal planes (*a*, *e*, *i*) out of those shown in the camera lucida reconstructions of *B* and *C*. The asterisks on the prelunate gyrus mark the extent of the injection site hidden in the banks of the superior temporal sulcus.
B: Camera lucida drawing of the lateral geniculate body at the level of section *e*.
C: Reconstruction of the pregeniculate nucleus. The stereotaxic planes are indicated near the rostral most (*a*) and the caudal-most (*i*) frontal sections of the nucleus.
Abbreviations as in Fig. 2.

incerta. This region of the PGn is sometimes considered as a separate nucleus and named the parageniculate nucleus (18). In this structure most of the silver grains were arranged in a fiber-like pattern (see Fig. 2 *C*, *h*, *i*). Autoradiographic material was also seen in the DLGn's magnocellular layers and their adjoining interlaminar zones (Fig. 2 *B*), the latter exhibiting the heaviest labeling. Only sparse fiber-like grain accumulations were seen in the parvocellular layers (Fig. 2 *B*). The same pattern of projection into the DLGn was found in a brain (Case 6) where one of the two foci of injections (6' in Fig. 1 *B*) partially overlapped that of Case 4, at the junction between the fundus and the upper bank of the STs. In Case 6, silver grains occupied the medial region of the caudal fourth of the PGn and the parageniculate nucleus.

Cases 7 and 8 received injections in the cortex of the caudal-most part of the STs, those injections being confined to its lower bank (see Fig. 1 *B*). By comparing adjacent sections alternately treated for autoradiography and myelin, the Case 7 and Case 8 injection sites appeared to lie mainly within the limits of the myeloarchitectonically distinguishable MT area. The LGb projections of these cases were very scarce. Labels were found in about 1 mm of the middle antero-posterior region of the PGn, this being restricted to its medial part. No labels were seen in the DLGn or in the parageniculate nucleus.

Case 5 showed a large injection site in the anterior part of the STs caudal half, involving the floor and a strip of both the lower and upper banks (see Fig. 1 *B*). As a result, labeled material was found in almost all the rostro-caudal extent of the PGn (Fig. 3 *C*). The most striking feature of this projection was the involvement of a band of the PGn which is immediately above the fibrous capsule surrounding the DLGn, whereas the dorsomedial and medial parts of the PGn were spared (Fig. 3 *C*, *b-g*). The pattern of silver grain distribution in the parageniculate nucleus (Fig. 3 *C*, *h*, *i*) was similar to that described in Case 4. The DLGn was completely devoid of label (Fig. 3 *B*).

DISCUSSION

Projections to the DLGn. Our results show that the visual areas of the STs around the MT project into the DLGn, but the MT itself does not, this being in agreement with Ungerleider *et al.* (25), who did not find the DLGn as a target of the MT efferents in macaque monkeys.

The distribution of the terminal fields in the DLGn's layers is nonhomogeneous, since the cortico-geniculate fibers arising from the STs terminate in the magnocellular layers of the DLGn with particular involvement of their interlaminar zones, completely sparing the parvocellular layers. A similar pattern of terminations in the DLGn has been previously described for fibers arising from area 18 in the macaque monkey (12), from areas 18 and MT in the owl monkey (13), and from the superior colliculus in both the New World (9) and the Old World monkeys (1). In searching for a possible functional role of this type of projection, it should be pointed out that dorsal lateral geniculate neurons with different functional properties are located within different layers. In particular, the Y-cells, typically activated by fast moving visual stimuli and which are possibly concerned in the discrimination of movement of visual stimuli (24), are esclusively located in the magnocellular layers (5, 21). It is therefore not surprising that extrastriate visual efferent arising from the cortical region bordering the MT, with neurons sensitive to the direction of moving visual stimuli, terminate in the magnocellular layers of the DLGn. However, it is quite surprising, in this respect that the MT of the macaque monkey does not project there, since it is regarded as the most specific visual area in motion analysis (17, 27).

Projections to the PGn. The PGn is known to receive cortical visual afferents in primates. In New World monkeys, some extrastriate visual areas, including the MT, are found to project into the PGn (7, 22). In the macaque monkey, mention should be made of the pioneering study of Campos-Ortega (4) who observed few degenerating fibers in the PGn after lesion of the striate area and a consistent degeneration zone when the lesion affected the circumstriate cortex (areas 18 and 19). As to extrastriate visual projections to the PGn arising from the banks of the STs, the bulk of the findings are concerned with efferents from the MT (16, 25) rather than from the surrounding areas. Our data shows that the cortex of the caudal half of the STs projects into the PGn. Moreover, the location of the terminal fields within the PGn seems to be linked to the origin of the corticofugal fibers. The target of the efferents from the anterior part of the STs's caudal half lies laterally and closer to the fibrous perigeniculate capsule when compared with the target of the efferents from the posterior part of the caudal half of this sulcus. This connectional distinction within the PGn fits in well with the cytoarchitectonic subdivision of the nucleus in two parts, called the internal and external layers according to the nomenclature of Niimi *et al.* (18). The internal layer, known to receive projections from the visual cortex (10, 22), is situated medially and in part dorsally to the external layer, which in turn lies just above the fibrous capsule of the DLGn and receives a retinal input (11) but not cortical visual afferents, at least in New World monkeys (7, 22). The cortex of the caudal-most part of the STs, which belongs to the visual region, turns out to be connected with the internal layer (present results), in agreement with the linkage pattern between visual cortical areas and the PGn (10, 22). On the contrary, the anterior part of the STs's caudal half appears to project into the external, retinorecipient layer of the PGn. This is what occurs in Case 5, whose injection site involved part of the superior temporal polysensory region, as proved by the autoradiographic material that was also found in the medial geniculate nucleus and in the inferior colliculus (unpublished results). Both these structures were free of labeling in Case 6, whose injection site partially overlapped that of Case 5, but whose projection target in the PGn was solely the internal layer. We can therefore infer that the peculiar projection zone in the external layer seen in Case 5 should be ascribed to the polysensory region of the STs.

The MT projection to the PGn in the macaque requires some further considerations. Previously described by Maunsell and Van Essen (16), this projection has been recently reported as doubtful by Ungerleider *et al.* (25), since it was present in only one out of five cases. Our results indicate that the two brains injected in the MT (Cases 7 and 8) each exhibited a light projection in the same zone of the PGn as case number MT-2 of Ungerleider *et al.* (25). Therefore, it is likely that the MT does project into the PGn. The scantiness of the projection zone may be due to the fact that our injection sites did not involve the entire MT. However, on the basis of the reconstructions of the Case 7 and Case 8 injection sites, the possibility that such a projection may be due to the involvement of the visual region just outside the MT cannot be completely ruled out.

The functional significance of the projection system from the STs cortex to the PGn is a matter of speculation. This is in part because the role of the PGn in the visual system is still a debated problem. Electrophysiological investigations showed that the firing of most of the PGn neurons is guided both by saccadic eye movements (even in the dark: 3, 14) and by light flashes (3). In other words, the PGn may be regarded as being a region of visual and oculomotor interaction (see also Ref. 3). Keeping in mind the involvement of the visual STs region in the analysis of moving visual stimuli, one might speculate that the pregeniculate afferents arising from the caudal part of the STs contribute to supply this nucleus with visual information related to motion analysis.

SUMMARY

1. Cortical projections from the visual region and adjacent polysensory region of the superior temporal sulcus (STs) to the lateral geniculate body (LGb) were investigated in the macaque monkey using an autoradiographic tracing method.

2. Solutions of tritiated aminoacids were injected into different parts of the caudal half of the STs of five animals. A survival time of 7 days was allowed.

3. Labels were found in both subdivisions of the LGb: the dorsal lateral geniculate nucleus (DLGn) and the pregeniculate nucleus (PGn). In particular, part of the visual cortical region adjacent to the middle temporal area (MT) projects into the DLGn as well as the PGn, whereas the MT itself and the superior temporal polysensory region project into the PGn only.

4. Afferents to the DLGn terminate in the magnocellular layers and in their adjoining interlaminar zones, completely sparing the parvocellular layers.

5. Afferents to the PGn terminate in separate regions of this nucleus; the MT and adjacent visual cortices project into the internal layer of the PGn, whereas the polysensosy region of the STs projects into the external retinorecipient layer of the PGn.

6. Possible functional implications of these projections are discussed.

Acknowledgements. — This investigation was supported by grants from the CNR and the Ministero Pubblica Istruzione, Rome, Italy.

REFERENCES

1. Benevento, L. A. and Fallon, J. H. The ascending projections of the superior colliculus in the rhesus monkey (*Macaca mulatta*). *J. comp. Neurol.*, **160**: 339-362, 1975.
2. Bruce, C., Desimone, R. and Gross, C. G. Visual properties of neurons in a polysensory area in superior temporal sulcus of the macaque. *J. Neurophysiol.*, **46**: 369-384, 1981.
3. Buttner, U. and Fuchs, A. F. Influence of saccadic eye movements on unit activity in simian lateral geniculate and pregeniculate nuclei. *J. Neurophysiol.*, **36**: 127-141, 1973.
4. Campos-Ortega, J. A., Hayhow, W. R. and De V. Cluver, P. F. The descending projections from the cortical visual fields of *Macaca mulatta* with particular reference to the question of a cortico-lateral geniculate-pathway. *Brain Behav. Evol.*, **3**: 368-414, 1970.
5. Dreher, B., Fukada, Y. and Rodieck, R. W. Identification, classification and anatomical segretation of cells with X-like and Y-like properties in the lateral geniculate nucleus of Old World primates. *J. Physiol., Lond.*, **258**: 433-452, 1976.
6. Gattass, R. and Gross, C. G. Visual topography of striate projection zone [MT] in posterior temporal sulcus of the macaque. *J. Neurophysiol.*, **46**: 621-638, 1981.
7. Graham, J., Lin, C.-S. and Kaas, J. H. Subcortical projections of six visual cortical areas in the owl monkey. *J. comp. Neurol.*, **187**: 557-580, 1979.
8. Graham, J. Some topographical connections of the striate cortex with subcortical structures in *Macaca fascicularis. Exp. Brain Res.*, **47**: 1-17, 1982.
9. Harting, J. K., Casagrande, V. A. and Weber, J. T. The projection of the primate superior colliculus upon the dorsal lateral geniculate nucleus: autoradiographic demonstration of interlaminar distribution of tectogeniculate axons. *Brain Res.*, **150**: 593-599, 1978.
10. Hendrickson, A. The pregeniculate nucleus of the monkey. *Anat. Rec.*, **175**: 341, 1973.
11. Hendrickson, A., Wilson, M. E. and Toyne, M. J. The distribution of optic nerve fibers in *Macaca mulatta. Brain Res.*, **23**: 425-427, 1970.
12. Hendrickson, A., Wilson, J. R. and Ogren, M. P. The neuroanatomical organization of pathways between the dorsal lateral geniculate nucleus and visual cortex in Old World and New World primates. *J. comp. Neurol.*, **182**: 123-136, 1978.
13. Lin, C. S. and Kaas, J. H. Projections from cortical visual areas 17, 18, and MT onto the dorsal lateral geniculate nucleus in owl monkeys. *J. comp. Neurol.*, **173**: 457-474, 1977.
14. Magnin, M. and Fuchs, A. F. Discharge properties of neurons in the monkey thalamus tested with angular acceleration, eye movement and visual stimuli. *Exp. Brain Res.*, **28**: 293-299, 1977.
15. Maioli, M. G., Squatrito, S., Battaglini, P. P., Rossi, R. and Galletti, C. Projections from the visual cortical region of the superior temporal sulcus to the striatum and claustrum in the macaque monkey. *Arch. ital. Biol.*, **121**: 259-266, 1983.
16. Maunsell, J. H. R. and Van Essen, D. C. The connections of the middle temporal visual area in the macaque monkey. *Soc. Neurosci. Abstr.*, **8**: 811, 1982.
17. Maunsell, J. H. R. and Van Essen, D. C. Functional properties of neurons in middle temporal visual area of the macaque monkey. I. Selectivity for stimulus direction, speed, and orientation. *J. Neurophysiol.*, **49**: 1127-1147, 1983.
18. Niimi, K., Kanaseki, T. and Takimoto, T. The comparative anatomy of the ven-

tral nucleus of the lateral geniculate body in mammals. *J. comp. Neurol.*, **121**: 313-323, 1963.

19. Polyak, S. *The Vertebrate Visual System.* Chicago Ill., Univ. Chicago Press, 1390 pp., 1957.
20. Seltzer, B. and Pandya, D. N. Afferent cortical connections and architectonics of the superior temporal sulcus and surrounding cortex in the rhesus monkey. *Brain Res.*, **149**: 1-24, 1978.
21. Shapley, R., Kaplan, E. and Soodak, R. Spatial summation and contrast sensitivity of X and Y cells in the lateral geniculate nucleus in the macaque. *Nature*, **292**: 543-545, 1981.
22. Spatz, W. B. and Tigges, J. Studies on the visual area MT in primates. II. Projection fibres to subcortical structures. *Brain Res.*, **61**: 374-378, 1973.
23. Squatrito, S., Galletti, C., Battaglini, P. P. and Riva Sanseverino, E. Bilateral cortical projections from cat visual areas 17 and 18. An autoradiographic study. *Arch. ital. Biol.*, **119**: 1-20, 1981.
24. Stone, J. and Dreher, B. Parallel processing of information in the visual pathways. A general principle of sensory coding? *Trends Neurosci.*, **5**: 441-446, 1982.
25. Ungerleider, L. G., Desimone, R., Galkin, T. W. and Mishkin, M. Subcortical projections of area MT in the macaque *J. comp. Neurol.*, **223**: 368-386, 1984.
26. Van Essen, D. C., Maunsell, J. H. R. and Bixby, J. L. The middle temporal area in the macaque: myeloarchitecture, connections, functional properties and topographic organization. *J. comp. Neurol.*, **199**: 293-326, 1981.
27. Zeki, S. M. Functional organization of a visual area in the posterior bank of the superior temporal sulcus of the rhesus monkey. *J. Physiol., Lond.*, **326**: 549-573, 1974.

Archives Italiennes de Biologie, 122: 311-319, 1984.

PROJECTIONS FROM THE EDINGER-WESTPHAL COMPLEX OF MONKEYS AS STUDIED BY MEANS OF RETROGRADE AXONAL TRANSPORT OF HORSERADISH PEROXIDASE

H. SEKIYA[1,3], K. KAWAMURA[1] AND S. ISHIKAWA[2]

Department of Anatomy, School of Medicine,
Iwate Medical University, Morioka 020, Japan[1]
and Department of Ophthalmology, School of Medicine, Kitasato University,
Sagamihara 228, Japan[2]

INTRODUCTION

The Edinger-Westphal nucleus (EW) is divided into two main parts: the medial and lateral visceral cell columns. The medial column is composed of large and small cells and the lateral column mostly of small cells. The rostral part of EW extends to the anteromedian nucleus (AM), which is composed mostly of small cells.

In confirming the previous study of Warwick (18), Burde and Loewy (3) recently demonstrated the AM/EW projection to the ciliary ganglion with the horseradish peroxidase method in the monkey, and projection to the spinal cord has also been shown (3, 5).

It has also been reported in the cat that AM and EW project to the spinal cord, cerebellar nuclei and ciliary ganglion (4, 9, 10, 11, 12, 13, 15, 16, 17). Although the functional role of AM and EW remains unclear, several authors (7, 8) have suggested that AM is possibly correlated with the accomodation, while EW is related to the pupillary light reflex. Clinically, a disturbance of accomodation or convergence is associated with the trauma at the neck or occipital portion.

An attempt was made in the present study to identify preganglionic (AM/EW) neurons which send thair axons to the ciliary ganglion in Japanese monkey (*Macaca fuscata*). A comparison of the type and distribution of AM and EW neurons projecting to the ciliary ganglion with those to the cerebellar nuclei and spinal cord was a primary objective of the present study.

MATERIAL AND METHODS

Four monkeys were used in this investigation. Under Ketalar and Nembutal anesthesia, a small amount of a 50% HRP [w/v] suspension was injected into the ciliary ganglion, cerebellar nuclei, or spinal cord. The injections were performed by means of 1.0 μl Hamilton syringe with a glass-micropipette, and the needle was kept in situ for 20 min.

The surgical approach to the ciliary ganglion was performed through an open space made between the superior and the lateral rectus muscles after the orbitofrontal cra-

---

[3] Present address: Dept. of Ophthalmology, School of Medicine, Kitasato University.

niotomy. In order to avoid the leakage of the enzyme injected into the ciliary ganglion, the surface of the ganglion was sealed with super glue (Alon Alpha). Injection of enzyme into the cerebellar nuclei (stereotactically) or the cervical spinal cord (under visual guidance) was made after removal of the bone and incision of the dura mater.

The animals were perfused intracardially with physiological saline followed by a mixture of 0.5% paraformaldehyde and 2.5% glutaraldehyde in 0.1M phosphate buffer (pH. 7.3). The fixative was washed out by perfusing a solution of 10% sucrose buffer. The brain was dissected free from the skull and stored in the phosphate buffer containing 30% sucrose, then it was cut transversally at 50 μm on a freezing microtome. Every third section was incubated according to the methods of Mesulum (14). Sections were counterstained with 1% neutral red. These were examined under the microscope, and locations of labeled neurons appearing in AM, EW and their adjacent structures were entered in the drawings of sections. Camera lucida drawings of the labeled cells in part of EW were also made. One monkey (Com 58), which received no injection of HRP into the brain, was used as a control to exclude endogenous reactivity of the enzyme in the AM and EW neurons.

Abbreviations.

AM: Anteromedian nucleus.
c.g.: Ciliary ganglion.
c.n.: Cerebellar nuclei.
CTF: Central tegmental field.
CV: Capillary vessel.
EW: Edinger-Westphal nucleus.
FR: Fasciculus retroflexus.
MLF: Medial longitudinal fasciculus.
mNr: Magnocellular part of the red nucleus.
NB: Nucleus accessorius medialis of Bechterew.
ND: Nucleus of Darkschewitsch.
Nint: Interstitial nucleus of Cajal.
pNr: Parvocellular part of the red nucleus.
s.c.: Spinal cord.
III: Somatic oculomotor nucleus.

RESULTS

After injections of HRP into the ciliary ganglion, the cerebellar nuclei or the spinal cord, many labeled cells (Figs. 1 and 2) occurred in several mesencephalic structures, e.g. the AM, EW, and " Perlia's nucleus ", the interstitial nucleus of Cajal, and the red nucleus. For the nomenclature and subdivisions of the visceral nuclei of the oculomotor complex, those of Carpenter and Peter (6) were used.

In *monkey Com 50* (2 points of 0.25 μl, sacrificed after 48 hours, Fig. 2), injections of HRP were made into the left cerebellar nuclei, which resulted in the staining of all parts of the nuclei on the left side as well as extensive areas of the right fastigial nucleus. In addition, the cerebellar cortex of the posterior vermis was partially stained. In the rostral mesencephalon, labeled cells appeared bilaterally in both AM and EW with ipsilateral preponderance. The number of the labeled cells in

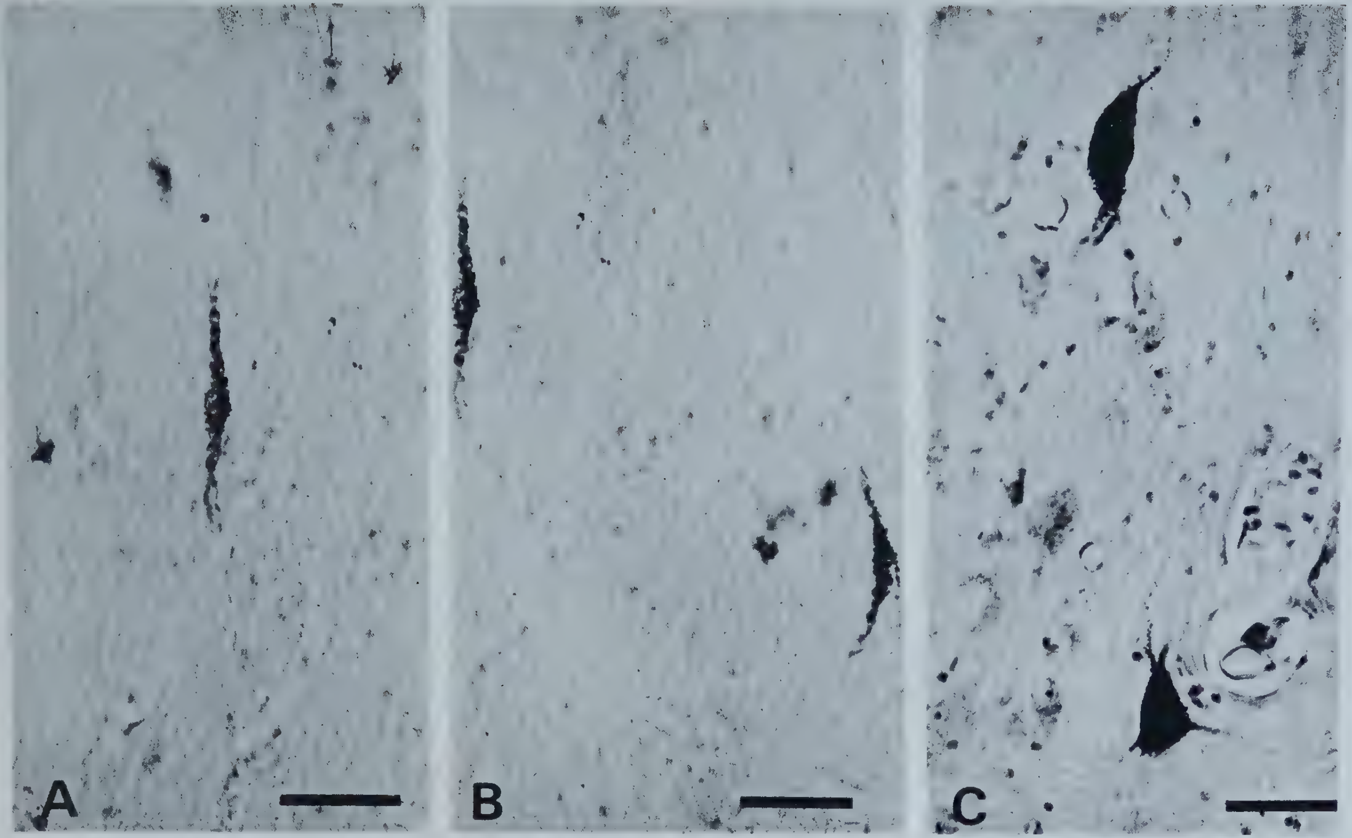

Fig. 1. – *Photomicrographs of retrogradely labeled cells in EW after injectins of HRP into the cerebellar nuclei (A), spinal cord (B) and ciliary ganglion (C) at the level C indicated in Fig. 2.*

Bright-field illumination. Scale bar: 50 μm.

AM and EW was 140 on the left and 72 on the right side. Labeled neurons were found in both the medial and lateral parts of AM, and in the medial and lateral visceral cell columns in EW (Fig. 3 *A*). A large number of the cells were spindle shaped (8-11 μm in diameter, the smaller diameter being measured for the spindle-shaped cell). A small number of cells of round/oval shaped (10-15 μm in diameter) were also labeled in the lateral visceral cell column of the caudal part of EW. In

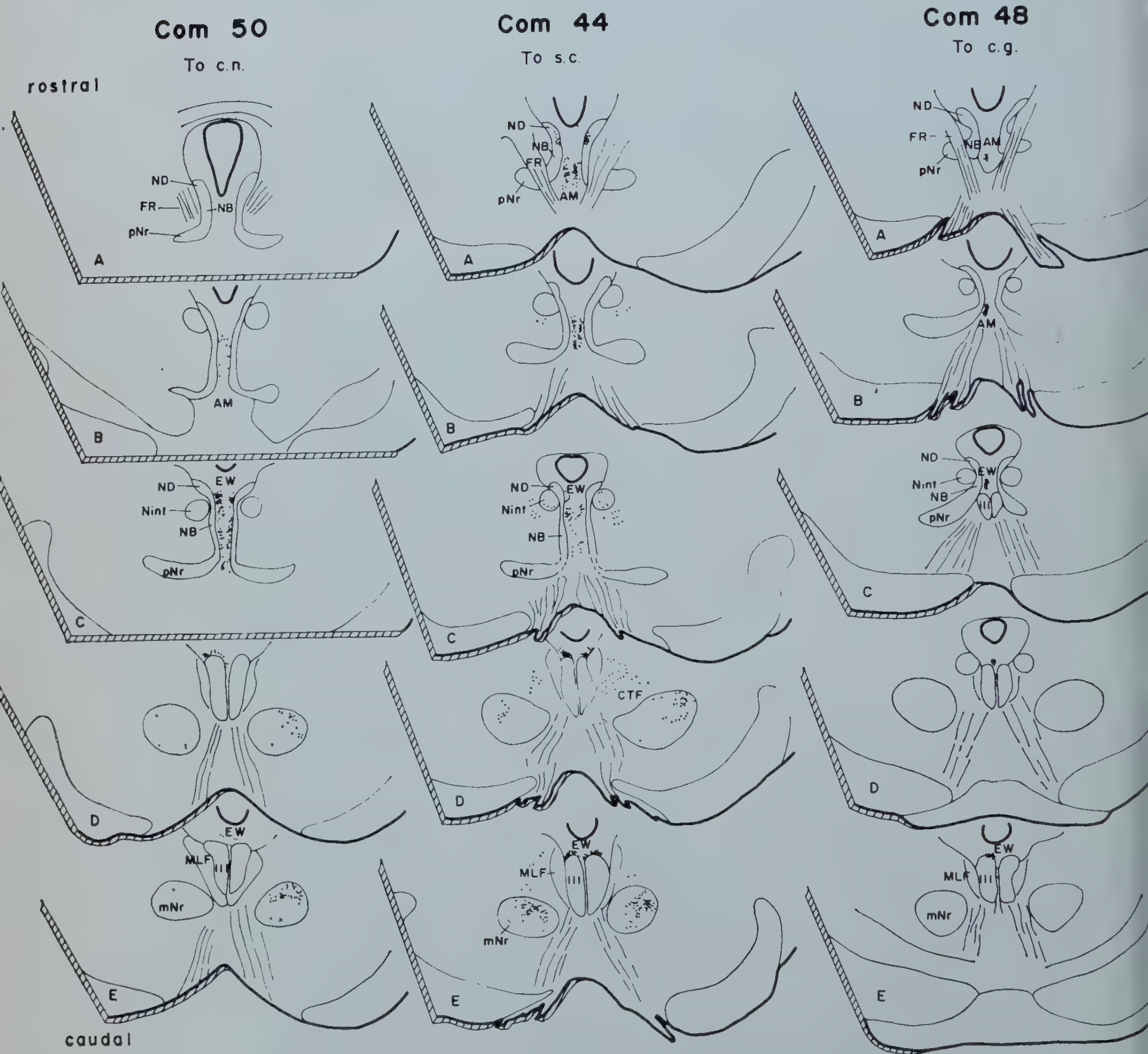

Fig. 2. – *Semidiagrams of five different levels (A, B, C, D, and E) of transverse sections through the midbrain, showing the distribution of labeled cells (dots) after injections of HRP into the left cerebellar nuclei (c.n., Com 50), the spinal cord (s.c., Com 44) and the left ciliary ganglion (c.g., Com 48).*

Labeled neurons in three neighboring sections are superimposed in the drawings.

the red nucleus, many large labeled cells were observed contralaterally, and only a few ipsilaterally, in the dorsal and lateral parts of the magnocellular region.

In *monkey Com 44* (6×0.3 μl, 48 h, Fig. 2), bilateral injections of HRP were made in the C4 segment of the spinal cord, which resulted in the staining of the enzyme covering C2-C7. In the rostral mesencephalon, labeled cells appeared in AM and EW on both sides. They were found in the entire part of the nuclei. A large number of labeled cells were spindle shaped (8-11 μm). A smaller number of labeled cells, round or oval in shape (10-15 μm), were located in the lateral visceral cell column of the caudal part of EW. Neurons were also labeled bilaterally in the nucleus of Darkschewitsch and the interstitial nucleus of Cajal, the lateral part of the magnocellular part of the red nucleus, and the central tegmental field.

In *monkey Com 48* (0.3 μl, 48 h, Fig. 2), injection of HRP was made into the left ciliary ganglion. Retrogradely labeled cells were found ipsilaterally in AM and EW. Labeled cells were large (25-40 μm) and oval or round. They were found in the medial part of AM and the medial cisceral cell column of EW (Fig. 3B). No labeled cells occurred in the lateral visceral cell column of EW. A few cells were also labeled in the nucleus of Perlia. In the caudal mesencephalon, however, the red nucleus and its adjacent structures contained no labeled cells.

In *monkey Com 58* (control case), no endogenous peroxidase activity was shown in the neurons of AM/ EW and adjacent structures.

DISCUSSION

With the aid of modern tracer techniques, AM and EW have recently been shown to send fibers to several structures, e.g. the spinal cord, cerebellar nuclei and ciliary ganglion. Projections to AM and EW have also been shown, autoradiographically by Benevento *et al.* (2) to originate from the sublentiform and olivary nuclei of the monkey pretectum: the former projects bilaterally to both AM and EW and the latter contralaterally to the lateral visceral cell column only.

In the following, projections to the three main targets, *i.e.* the cerebellum, spinal cord and ciliary ganglion will be discussed. Projections from the midbrain structures other than the AM and EW will not be considered here.

Projections to the cerebellum. Direct projections from AM and EW to the cerebellar nuclei has been demonstrated with the HRP method in the cat (16). Labeled cells in the cat were small to medium sized, oval or spindle-shaped, and they were found bilaterally in almost the entire parts of AM and EW with a contralateral preponderance. The present study also demonstrated in the monkey that the AM and EW neurons project to the cerebellar nuclei[1]. Projection neurons to the cerebellum were spindle-form of small sized (8-11 μm), and they were distributed throughout AM and EW (Figs. 1 *A* and 3 *A*). Small, round neurons (11-15 μm) were also labeled in the lateral visceral cell column of the caudal part of EW.

---

[1] Since parts of the cerebellar cortex was also stained with the enzyme in our experiment (see Results), the possibility remained that projections to the cortex, if existed, might have been included in our data.

Although the definite conclusion could hardly be deduced from our experiment, due to the partial spread of the injected HRP to the contralateral fastigial nucleus, it appears that the projection is bilateral with an ipsilateral preponderance as counted the number of labeled cells in monkey Com 50, which is at variance with the findings of cats (16).

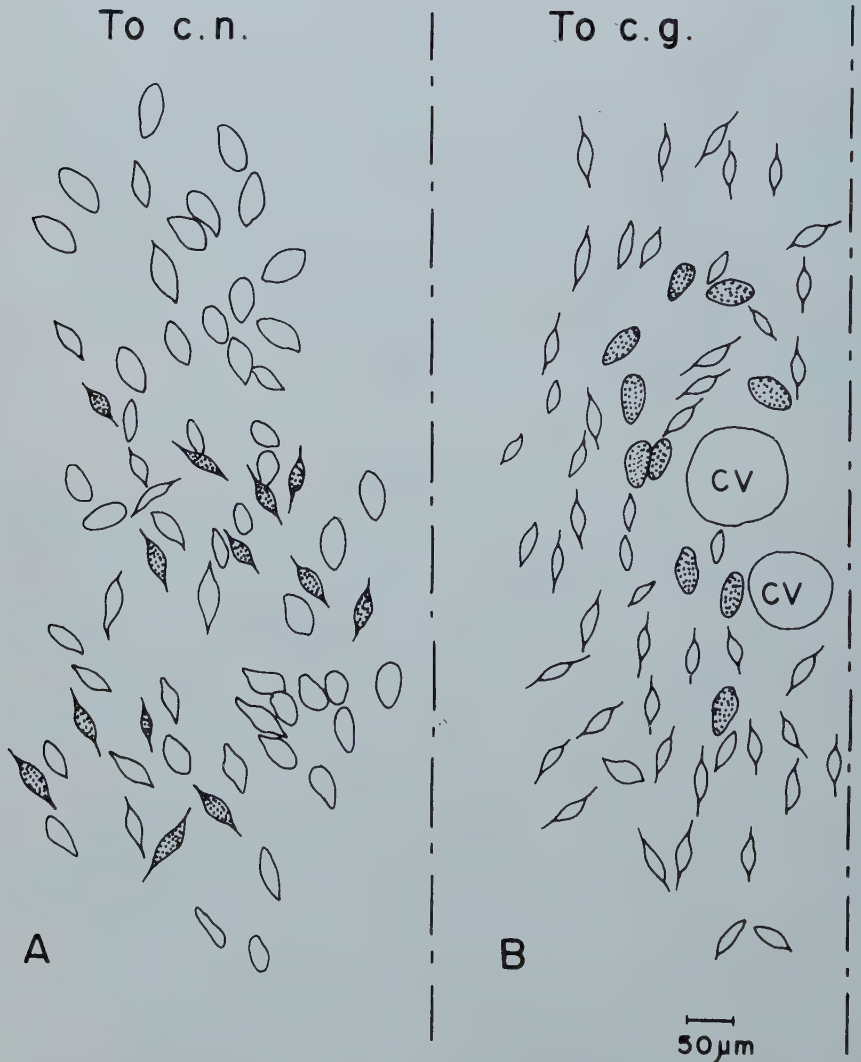

Fig. 3. – *Camera lucida drawings of labeled cells (stippled) on the left sides of a section through the visceral nuclei of the oculomotor complex (at level C of Fig. 2) after injection of HRP into the cerebellar nuclei (A) and the ciliary ganglion (B).*

Note that the level of B is about 0.3 mm rostral to that of A. Outlines of non-labeled cells are also traced. Broken lines indicate the midline. Scale bar 50 μm.

Projections to the spinal cord. Spinal projection neurons in AM and EW have been identified in the cat (16, 17) and monkey (3, 5). The present study confirmed the previous findings. Thus, projection neurons to the spinal cord were spindle-form of small sized (8-11 μm), and they were distributed in the entire parts of AM and EW (Fig. 1 *B*). Small round neurons (10-15 μm) were also found to give rise to the projection from the lateral visceral cell column of the caudal part of EW.

As seen above, the distribution of neurons and their cell-type which project to the spinal cord or the cerebellum were quite similar in the monkey. As described previously by Sugimoto *et al* (16), however, there was a clear difference in the distribution of the two kinds of the projection neurons in AM/EW, although the cell-types were similar between the two.

Projections to the ciliary ganglion. After the ciliary ganglionectomy in the monkey, Warwick (18) observed retrograde cellular degeneration (chromatolysis, swelling and nuclear eccentricity) in AM and EW on the ipsilateral side. Larger cells (37-45 μm as measured from his figure 10) of round/oval form were frequently found to be affected. He (18) also obtained findings from lesion experiments which led him to conclude that 97% of the ciliary ganglion cells relate to the ciliary muscle and 3% to the iris sphincter. Jampel and Mindel (8) could later produce iris-bulge and changes in the retinoscopic reflex (accomodation) after electrical stimulation of the monkey AM.

In the monkey, as described first in the present study, neurons projecting to the ciliary ganglion were large (25-40 μm) and oval/round in shape, and were located ipsilaterally in the medial part of AM and the medial visceral cell column of EW as well as in the " Perlia's nucleus ". The size, shape and distribution of the cells projecting to the ciliary ganglion (Figs. 1 *C* and 3 *B*) were clearly different from those projecting to the cerebellum (cp. Figs. 1 *A* and 3 *A*) or the spinal cord (cp. Fig. 1 *B*). It is apparent that the neurons projecting to the ciliary ganglion are larger than those going to the cerebellum or the spinal cord. This is in accord with the findings of the double labeling method performed in the cat by Burde *et al.* (4) and Maciewicz *et al.* (13). They showed that the neurons projecting to the ciliary ganglion do not share axon collaterals with those projecting to the cerebellum or spinal cord, whereas some cells share collaterals between the cerebellar and spinal projection neurons.

The present findings thus confirmed and further extended the previous data (1, 3) in showing the distribution of the projection neurons. It may be assumed that in the monkey large and oval/round cells in the medial part of AM and the medial visceral cell column in EW, which may receive visual inputs from the pretectal nuclei (2), are responsible for the accomodation and pupillary constriction.

SUMMARY

By means of retrograde axonal transport of horseradish peroxidase, an experimental study was made in the Japanese monkey of the projection from the anteromedian

nucleus (AM) and Edinger-Westphal nucleus (EW) to the ciliary ganglon, cerebellar nuclei and spinal cord. Special attention was paid on the labeled cell forms.

Neurons projecting to the cerebellar nuclei or the spinal cord were small (8-11 μm in diameter) and spindle-shaped, and they were located in almost the entire parts of both AM and EW. On the other hand, cells which gave off their axons to the ciliary ganglion were large (25-40 μm in diameter) and oval/round in shape. Their locations were confined to the medial parts of both AM and EW, except for the most caudal part of EW. In addition, a few cells in the " nucleus of Perlia " were found to project to the ciliary ganglion.

Acknowledgements. — We thank Dr. K. Mukuno for his kind help in the operation of the ciliary ganglion.

REFERENCES

1. Akert, K., Glicksman, M. A., Lang, W., Grob, P. and Huber, A. The Edinger-Westphal nucleus in the monkey. A retrograde tracer study. *Brain Res.*, **184**: 491-498, 1980.
2. Benevento, L. A., Rezak, M. and Santos-Anderson, R. An autoradiographic study of the projections of the pretectum in the rhesus monkey (Macaca mulatta): evidence for sensorimotor links to the thalamus and oculomotor nuclei. *Brain Res.*, **127**: 197-218, 1977.
3. Burde, R. M. and Loewy, A. D. Central origin of oculomotor parasympathetic neurons in the monkey. *Brain Res.*, **198**: 434-439, 1980.
4. Burde, R. M., Parelman, J. J. and Luskin, M. Lack of unity of Edinger-Westphal nucleus projections to the ciliary ganglion and spinal cord: a double-labeling approach. *Brain Res.*, **249**: 379-382, 1982.
5. Castiglioni, A. J., Gallaway, M. C. and Coulter, J. D. Spinal projections from the midbrain in monkey. *J. comp. Neurol.*, **178**: 329-346, 1978.
6. Carpenter, M. B. and Peter, P. Accessory oculomotor nuclei in the monkey. *J. Hirnforsch.*, **12**: 405-418, 1970-1971.
7. Chin, N. B., Ishikawa, S., Lappin, H., Davidowitz, J. and Breinin, G. M. Accomodation in monkeys induced by midbrain stimulation. *Invest. Ophtalmol.*, **7**: 386-396, 1968.
8. Jampel, R. S. and Mindel, J. The nucleus for accommodation in the midbrain of the macaque. *Invest. Ophtalmol.*, **6**: 40-50, 1967.
9. Kuypers, H. G. J. M. and Maisky, V. A. Retrograde axonal transport of horseradish peroxidase from spinal cord to brain stem cell groups in the cat. *Neurosci. Lett.*, **1**: 9-14, 1975.
10. Kuypers, H. G. J. M. And Maisky, V. A. Funicular trajectories of descending brain stem pathways in cat. *Brain Res.*, **136**: 159-165, 1977.
11. Loewy, A. D. and Saper, C. B. Edinger-Westphal nucleus: projections to the brain stem and spinal cord in the cat. *Brain Res.*, **150**: 1-27, 1978.
12. Loewy, A. D., Saper, C. B. and Yamodis, N. D. Re-evaluation of the efferent projections of the Edinger-Westphal nucleus in the cat. *Brain Res.*, **141**- 153-159, 1978.
13. Maciewicz, R., Phipps, B. S., Foote, W. E., Aronin, N. and DiFiglia, M. The distribution of substance P-containing neurons in the cat Edinger-Westphal nucleus: relationship to efferent projection system. *Brain Res.*, **270**: 217-230, 1983.
14. Mesulam, M.-M. Tetramethyl benzidine for horseradish peroxidase neurohisto-

chemistry: a non-cardinogenic blue reaction-product with superior sensitivity for visualizing neural afferents and efferents. *J. Histochem. Cytochem.*, **26**: 106-117, 1978.

15. Sugimoto, T., Itoh, K. and Mizuno, N. Localization of neurons giving rise to the oculomotor parasympathetic outflow: a HRP study in cat. *Neurosci. Lett.*, **7**: 301-305, 1977.
16. Sugimoto, T., Itoh, K. and Mizuno, N. Direct projections from the Edinger-Westphal nucleus to the cerebellum and spinal cord in the cat: an HRP study. *Neurosci. Lett.*, **9**: 17-22, 1978.
17. Toyoshima, K., Kawana, E. and Sakai, H. On the neuronal origin of the afferents to the ciliary ganglion in cat. *Brain Res.*, **185**: 67-76, 1980.
18. Warwick, R. The ocular parasympathetic nerve supply and its mesencephalic sources. *J. Anat., Lond.*, **88**: 71-93, 1954.

INSTRUCTIONS TO AUTHORS

Submission of a paper will be taken to imply that it has not previously been published, except in abstract form, and that it is not being considered for publication elsewhere. Decision as to publication of papers submitted to the *Archives Italiennes de Biologie* will be based on the opinion of the Editorial Board as to the significance and originality of the work.

Address for Manuscripts: Chief Editor, Archives Italiennes de Biologie, Istituto di Fisiologia Umana, Via S. Zeno 31, 56100 Pisa, Italy. The books to be reviewed should also be sent to the same address.

Form of Manuscripts: Manuscripts should be submitted in duplicate and typed in double spacing. There should be a separate title page with: *a*) the title, *b*) the authors' names, *c*) the laboratory of origin, with complete address of each author, *d*) a running title, and *e*) the address to which proofs should be sent.

The main body of full-length papers should be divided into: 1) Introduction, 2) Methods, 3) Results, 4) Discussion, 5) Summary (French manuscripts should be accompanied by an English summary), 6) Acknowledgements, 7) References. Short communications should neither be divided in sections nor is the abstract required; the text should not be longer than 4 printed pages, including tables and illustrations. Review articles must have an initial Table of Contents and a final Summary. Book Reviews should not be longer than one printed page.

References should be typed in a numbered list, alphabetically arranged on a separate sheet and double spaced. The style of citation should conform to that used in this issue of the Archives. The number appropriate to each reference should be included in parentheses at the appropriate point in the text. " Personal communications " and " unpublished observations " should not be cited in the list of references, but may be noted in parentheses in the text.

Figures: Illustrative material should be presented in the form of sharp and contrasty photographic prints on glossy paper suitable arranged and mounted to form a complete figure. Original figures may also be accepted. All illustrations, accompanied by separate legends to be used by the printer, must be submitted in duplicate and labeled lightly in black pencil on the back, indicating: *a*) top of the figure, *b*) figure number, *c*) authors name. The size of lettering should be chosen to be proportionate to the size of the illustration after reduction, and so the smallest elements will be legible when reduced. Lettering and symbols should be kept within the frame of the figure, to limit the degree of reduction. Very small dots and fine lines should be avoided since they may be lost in reproduction.

Tables: Tables of numerical data should each be typed with double spacing on separate pages numbered in sequence in Roman numerals, provided with a heading, and referred to in the text, as Table I, Table II, etc.

Legal requirements: Papers describing animal experiments must be conducted in conformity with the legal requirements. Evidence should be provided by the Authors that they took adequate steps to ensure that animals did not suffer. Papers describing experiments on human subjects should be conducted in conformity to the Code of Ethics of the World Medical Association (Declaration of Helsinki).

Page charge: A page charge of U.S. $ 5.00 or Lire 7.500 for printed page is imposed to cover part of the cost of publication. Editorial consideration of a paper is not related to the acceptance of the page charge, which is expected to be paid by the author's research funds or the institution that supported the research.

Proofs and reprints: Proofs should be corrected and returned promptly to the Chief Editor. Corrections should be kept to a minimum. Reprints can be supplied only if ordered at the time in which proofs are returned by the Author. Unless specified, the invoice will be sent to the Author to whom the proofs were addressed.

Copyright: Upon acceptance of a paper the entire copyright shall pass to the University of Pisa. Request for permission to reproduce any part of papers published in Archives Italiennes de Biologie should be addressed to the Administration of the Archives. The Chief Editor will normally grant all requests from authors to reproduce material from their own papers. Request of permission must be accompanied by the consent of the Authors concerned.

Archives Italiennes de Biologie

VOLUME 122 NUMBER 4 DECEMBER 1984

CONTENTS

RESEARCH PAPERS

KEMALI, M. *and* GUGLIELMOTTI, V. The distribution of substance P in the habenulo-interpeduncular system of the frog shown by an immunohistochemical method *Page* 269

YAMAUCHI, T., NEWMAN, S. E. *and* AJMONE-MARSAN, C. Experimental studies on different thresholds for epileptiform activity 281

MAIOLI, M. G., GALLETTI, C., SQUATRITO, S., BATTAGLINI, P. P. *and* RIVA SANSEVERINO, E. Projections from the cortex of the superior temporal sulcus to the dorsal lateral geniculate and pregeniculate nuclei in the macaque monkey 301

SEKIYA, H., KAWAMURA, K. *and* ISHIKAWA, S. Projections from the Edinger-Westphal complex of monkeys as studied by means of retrograde axonal transport of horseradish peroxidase 311

Managing Editor: Prof. O. Pompeiano

Printed by A. Paoletti Comp., 50015 Grassina, Firenze, Italy
Authorization of the Pisa Tribunal No. 20/1956
Arch. ital. Biol. ISSN: 0003-9829